



Shahrood University of
Technology



Iranian Society of
Mining Engineering
(IRSM)

Investigating Effect of Liner Type and Lifter Count on Kinetic, Potential, and Total Energies of Grinding Media in Industrial Ball Mills–Part 1: Separate Lifters with Same Volumes

Mohammad Jahani Chegeni*, Sajad Kolahi, and Asghar Azizi

Faculty of Mining, Petroleum & Geophysics Eng., Shahrood University of Technology, Shahrood, Iran

Article Info

Received 24 July 2024
Received in Revised form 27
November 2024
Accepted 10 January 2025
Published online 10 January 2025

DOI: [10.22044/jme.2025.14802.2808](https://doi.org/10.22044/jme.2025.14802.2808)

Keywords

Discrete element method
Industrial ball mills
Liner type
Lifter count
Kinetic

Abstract

Consumed energy is the most important issue and concern in industrial ball mills, and includes a major part of the costs of mineral processing plants. By using suitable liners and the optimal lifter count, the energy of the mill is properly transferred to the balls. In Part 1 of this research work, five types of liners, i.e. Lorain, Osborn, Rib, cuboid, and Hi-lo, are examined. These liners all have separate lifters with the same volume. Their difference is in the width, height, and type of lifter profile. First, all types of liners are simulated with four lifters using the Discrete Element Method (DEM). Then the lifter count is increased four by four to fill the entire wall of the mill with lifters. Based on this, Lorain liner from 4 to 24 lifters, Osborn liner from 4 to 120 lifters, Rib liner from 4 to 40 lifters, and cuboid and Hi-lo liners from 4 to 64 lifters are simulated. For the first time, the kinetic (KE) and potential (PE) energies as well as the sum of these two energies (TE) of all the balls are calculated, and compared in the entire duration of the simulation from 0–13s for all the liner types and lifter counts mentioned above. Finally, by using data related to KE, PE, and TE for each type of liner, the optimal lifter count is obtained. Accordingly, 16 to 20 lifters are recommended for the Lorain liner, 64 to 76 lifters for the Osborn liner, 24 to 32 lifters for the Rib liner, 44 lifters for the cuboid liner, and 36 to 44 lifters for the Hi-lo liner.

1. Introduction

So far, a large quantity of mineral processing equipment has been simulated in laboratory, pilot, and industrial scales with the Discrete Element Method (DEM) such as various types of crushers, mills, hoppers, etc. In the present research work, only ball mills have been investigated, and other mills such as SAG, planetary, etc. have not been investigated. Therefore, they have not been mentioned in the literature review, and the research works conducted on them have not been reviewed. Also a great deal of research work, in which wear of liners in all types of mills has been investigated, has not been considered here. Also various parameters of ball mills have been investigated by far, such as the rotation speed of the mill, its filling level, feed size distribution, dimensional distribution of mill balls, wear of liners, particle breakage, particle shape etc. which once more are not relevant to the issues raised here, and are therefore not addressed. But in the current research

work, only the effect of liner type and lifter count on the *KE*, *PE*, and *TE* of the balls in industrial ball mills has been investigated. According to the above, the literature was reviewed.

Nowadays, the obligation to enhance and sustain the throughputs of grinding mills over a longer time, while lessening the operating costs is of primary concern in milling industries [1]. Therefore, an efficient grinding operation enlarges the production level, and is a requirement for advancing the energy efficiency of the whole mineral processing procedure. [2]. Ball mills have been utilized predominantly in mineral processing industry since the mid of 19th century due to the requisite for finer material. However, there is still need for perception of the combined and individual effects of all design and operating variables to make the whole process more efficient [3].

✉ Corresponding author: M.Jahani@shahroodut.ac.ir (M. Jahani Chegeni)

Liners play a crucial role in the ball milling process, due to their strong influence on load motion and behavior [1]. The Discrete Element Method (*DEM*) is emerging as a tool that holds possibilities for exploration of various liner profiles by simulation [1]. The common approach in designing liners is designing for a longer life. However, this approach does not necessarily consider optimum performance over the liner life [4]. *DEM* simulation hitherto has been extensively applied as a leading tool to describe diverse issues in granular processes [5]. A good many of researchers have been working on simulating the tumbling ball mills using the *DEM* method. Mishra and Rajamani were the first ones who studied the trajectory of the balls in industrial-scale ball mills using *DEM*. They developed a computer code based on *DEM* to model the motion of the balls in a 55-cm diameter ball mill. The code incorporated a scheme to calculate the applied torque, and hence, power input to the mill. Two different liner cross-sections rectangular and triangular were simulated. They found that with a particular model for the friction coefficient, the predicted torque agreed well with the experiments [6]. In another collaborative study, Mishra and Rajamani conducted numerical simulation of charge motion in a 4.75 m diameter ball mill with thirty lifters using *DEM*. They simulated the ball mill with three different lifter-bar configurations: swivel, wavy, and rectangular. The face angle was varied from 90 to 145°, and the lifter height was kept slightly higher than the ball diameter. They showed that two important factors, i.e. the configuration of the liner and the geometry of the lifting surfaces, were correlated with the overall mill performance [7]. Once more, Mishra and Rajamani, in a couple of simultaneous studies, utilized *DEM* to simulate the charge motion in a 4.75 m diameter ball mill. At the first part, they compared the *DEM* simulation results with experiments: the trajectory of two balls, the positions of the toe and shoulder points, and the power draw. At the second part, it was shown that larger balls segregate to the center at high speeds and to the shell at lower speeds. The friction between the ball charge and the mill shell can increase the power draw. Also they concluded that simulation provides collision frequency information, which is the key to mill design and optimization [8, 9]. Agrawala et al. investigated the mechanics of media motion in a 90-cm diameter ball mill using *DEM*. They predicted the profile of the ball charge, impact energy distribution, and power draw as a function of mill operating conditions. The images of the charge motion were captured on a video camera, and analyzed with image-processing software. Simultaneously, the mill power was recorded with a torque sensor [10]. Radziszewski compared three modelling approaches to *DEM* implementation to charge motion modelling

inside a 12 m length ball mill with thirty-six lifters of two types of lifter profiles, i.e., rectangular Hi-lo lifters and 60° Hi-lo lifters. Simulations conducted for different mill speeds (65%, 75%, and 85% CS) and different charge volumes (20% and 30%). All three approaches were anchored in physical fundamentals of particle motion and produce broadly similar results to charge motions profiles [11]. Cleary, took advantage of *DEM* to anticipate consumed energy of industrial-scale ball mills, and to investigate their affectability to operating conditions such as charge composition, motion, and behavior, as well as lifter geometry [12,13]. Also Cleary simulated a 5 m diameter ball mill using *DEM* and predicted particle flows inside the mill. Charge behavior, torque, and power draw were analyzed for a range of rotation rates from 50 to 130 % of the critical speed for the mill. He found that higher grinding rates can be produced for lower fill levels, but the resulting mill throughput is too low to be useful [14]. Monama and Moys investigated *DEM* modelling of the dynamics of ball mill startup. A 0.55 m diameter ball mill was used to perform the experimental analysis. The mill had 12 cuboid lifters. They changed mill speed from 32 to 145% of critical speed. They concluded that the dynamics of mill startup can be modeled with a fair accuracy using *DEM* [15]. Hlungwani et al. performed the validation of the results of *DEM* simulations by comparing them with charge motion in a transparent laboratory mill. They scrutinized the effects of liner profiles and mill speed on energy efficiency and mill capacity. Two types of square and trapezoidal lifter profiles were used to investigate mill power and charge behavior. *DEM* successfully predicted that the trapezoidal lifters draw more power than the square lifters. This means that the newly installed square lifters will give their best performance after some wear [16]. Djordjevic examined the influence of lifters on power draw of ball mills using *DEM*. Results obtained showed that lifter condition will have a significant influence on the power draw, and on the mode of energy consumption in the mill. Relatively high lifters will consume less power than low lifters, under otherwise identical conditions. The fraction of the power that will be consumed, as friction will increase as the height of the lifters decreases [17]. In another research work, Djordjevic compared power draw modelling results using the *DEM* with results derived from the widely used empirical model of Morrell. The results obtained confirmed that modelling of the power draw for a vertical slice of the mill, of thickness 20% of the mill length, is a reliable substitute for modelling the full mill [18]. One more time, Djordjevic calculated normal and shear stresses of lifters in ball mills using *DEM*. Results showed that for the modelled case, the magnitude of the stresses

decreases as the lifter count increases. In the two-lifter case, the shape of the charge is not visibly affected by the rotation of the mill. But for mills with 14 and 22 lifters, the shape of the charge is dramatically affected by the mill rotation [19]. Mishra reviewed computer simulation of tumbling mills by *DEM* in two parts. At the first part, he investigated contact mechanics, and evaluated the perceiving of the three important areas of the simulation aspect: the inter-particle force laws, significance and choice of contact parameters, and implementation of the numerical scheme. At the second part, he studied practical applications such as charge motion, power draw prediction, liner, and lifter design and microscale modeling for calculation of size distribution. He concluded that charge motion in ball mills can be computed with ease using *DEM*. Furthermore, He showed that power draw of ball mills can be predicted within 10% [20, 21]. Powell and McBride illustrated the media motion and grinding regions (head, departure shoulder, center of circulation, equilibrium surface, bulk toe, and impact toe) inside ball mills. They presented improved descriptions and definitions of the motion of grinding media in all tumbling ball mills, and created a more rigorous, meaningful, and consistent set of definitions of the grinding action in ball mills [22]. Makokha and Moys evaluated the effect of lifter profile design on the milling capacity and kinetics of batch grinding for optimizing ball-milling performance using mono-sized quartz as feed. They tested three lifter profiles: bevel with 45° lifter face angle to represent the worn lifters, bevel with 60° lifter face angle to represent the new lifters, and worn bevel modified with cone-lifters. They noted that the lifter profile significantly influences the production of fines and milling rate [23]. A unique way to optimize the performance and life of worn liners in industrial ball mills was presented by Makokha et al. They improved the liner performance and life using retrofits. They assessed the ability of *DEM* to model the effect of lifter profile on mill charge behavior, and hence its potential as a tool for optimizing the design of mill liners. Two liner profiles, bevel and bevel retrofitted with detachable cone-shaped lifters were utilized in their investigation [1]. Rezaeizadeh et al. showed that in order to achieve a higher impact mechanism and higher overall efficiency in ball mills, lifter height, mill rotation speed, and the lifter count should be increased, but the mill filling should be decreased. They also showed that the milling power has a linear relationship with the height and distance of the lifters (S/H) and the milling speed [24]. Pérez-Alonso and Delgadillo using digital image analysis presented an experimental validation of the ball mill *DEM* simulation for the velocity profiles of the balls, the shoulder and toe points, and the predicted power

draw. The experimental values were compared with the simulated ones using different lifter profiles and charge levels. The experimental and simulated values were very close, leading to the conclusion that such *DEM* predictions represent an accurate description of the process in ball mills [25]. In the early 1960s, Art MacPherson investigated the effect of lifter spacing to height ratios, and concluded a ratio of 4:1 maximized grinding [26]. Yahyaei et al. extended a method to design lifters of an industrial ball mill. They evaluated the mill performance via exploring the effect of lifter type. Therefore, five different lifter profiles were simulated, and compared to the present lifter. They concluded that by reduction of the lifter height from 300 mm to 210 mm, a lifter which had alike face angle as the present one can enhance the plant throughput about 8% with the same P_{80} as the current lifter [4]. Bbosa et al. developed a novel methodology to compute and determine power consumption of every size within a distribution of charge in ball mills. Experiments were performed utilizing glass bead charges, which were dry and spherical in a laboratory-scale ball mill. A torque sensor and a tachometer were installed on the mill, to provide calculations of power [27]. Boemer and Ponthot, utilizing *DEM*, simulated a 0.8 m diameter laboratory ball mill. At experimental tests for validation, they studied the influence of parameters such as charge motion and power draw. Also two different geometries of the shell liner were studied [28]. Peng et al. utilized mono-sized iron ore particles to simulate charge behavior within a 0.52 m ball mill with single wave liner profile and twelve lifters using *DEM*. They used the Design Of Experimental (*DOE*) method with two factors: the lifter height and mill speed. Using *DOE*, the *DEM* simulation conditions were defined. The results showed that the dependence of the impact toe and head on mill speed is higher than its dependence on the lifter height [29]. Bian et al., using *DEM* simulation, investigated the effect of ball mill rotation speed and lifter profiles on its torque and power draw as well as on particle behavior. Results indicated that the ball mill torque is affected by its rotation speed, lifter height, and lifter number. They also concluded that the changes in the torque and power draw is dependent on two significant factors, i.e. lifter and particle area ratio [30]. Sun et al. studied the *RPAS* liners in ball mills. They carried out numerical and experimental investigations on three types of *RPAS* liners including *QASL*, *PASL*, and *HASL*. Also single liner and multiple angle liners with different angles were assembled and compared. Results showed that the optimal structure of *RPAS* liners is *QASL* with an assembled angle of 50° [31]. Yin et al. investigated the impact mechanism between different charges and lifters in a laboratory-scale ball mill. The mill diameter was 520 mm, and its length

was 40 mm and equipped with twelve equally spaced and different height rows of rectangle lifters. They concluded that lifter height has a significant influence on the charge behavior. Increasing the lifter height increases the shoulder position and lifts the steel balls to the higher position [5]. Pedrayes et al. investigated frequency amplitude specification of torque in a pilot scale ball mill using *DEM*. They considered factors such as particle type, rotational speed of the mill, and its filling level. They showed that charge torque signal in pilot-scale ball mills includes adequate information to precisely specify the charge level of ball mills [32]. Li et al. studied the performance of a specific 900 mm × 1800 mm ball mill with liner structure based on *DEM*. They simulated five kinds of lifter profiles (triangular, trapezoidal, rectangular, ladder, and hemispherical). The results showed when the rectangular lifter was installed, the ball mill efficiency was significantly high. Also they studied the effects of the height–width ratio of the rectangular lifter, the height of the lifter and the lifter count on the working efficiency of the ball mill. It was found that a number of rectangular lifters of twelve and a height–width ratio of 3:1 produced the best results [33]. Panjipour and Barani, utilizing *DEM*, investigated the effect of ball size distribution on breakage mechanism, charge motion, and power draw of a 25 cm ball mill. The mill was simulated in different filling levels from 15 to 40%. Two types of balls with diameters of 2 and 2.5 were considered. The results demonstrated that at a constant filling level, the mill power draw fluctuated with fluctuation of the ball size distribution [34]. Rosales-Marín et al. evaluated the effect of face angle and wear of lifters, as well as mill rotation speed on power draw and breakage rate of a laboratory-scale ball mill. The results confirmed the phenomena that all the measured torque/power values decreased after a certain value of mill critical speed (75%) [3]. Lee et al. analyzed the grinding kinetics in a laboratory-scale 20 cm ball mill with six designed lifters (1 cm-4 lifters, 1 cm-8 lifters, 1 cm-12 lifters, 2 cm-4 lifters, 2 cm-8 lifters, 2 cm-12 lifters). Also they compared experimental and simulated product-size distributions for various grinding times for these six ball mills [2]. Li et al., utilizing *DEM*, investigated the breakage effect as well as charge motion of a ball mill with a magnetic lifter. They compared magnetic lifters to common rubber and steel ones, and demonstrated that the charge motion in the mill, while using magnetic lifters was chiefly cascading. Also they compared mill charge trajectories of various lifter types under different mill speeds (from 65% to 85% of critical speed) [35]. Chimwani and Bwalya using *DEM* investigated how shell liners can perform ball disjunction in ball mills. They simulated a ball mill with four sectors. Each sector had different lifter profiles. Three lifter profiles were used (45°, 75°, and

90°). Also three ball types with different sizes were tracked for proof of disjunction at 75% and 60% of mill critical speed. They found that varying axial lifter profile configuration can affect ball disjunction, especially for the mill running at 75% of critical speed [36]. Góralczyk et al. studied the enhancing power efficiency and yield of the grinding process in ball mills by indirect calculations of within dynamics. They presented a retroactive overview of the existing models of internal charge motion, an overview of the innovations in process control, and some recent research and industrial approaches from the power draw reduction point of view [37]. Shahbazi et al. presented a thorough review of the influence of various ball shapes (spherical, cylpebs, eclipsoids, cube, worn ball, boulpebs, conipebs) and geometries on the performance of ball mills. They studied grinding factors (kinetic energy, charge behavior, power draw, toe, shoulder, impact mechanism) and the particle size of product in ball mills. They observed that ball shape can influence the performance of a ball mill. The media can directly affect the breakage rate, mill charge behavior, power draw, and generally energy consumption [38]. AmanNejad and Barani carried out a broad survey to describe the role of mill rotation speed and ball size distribution as well as their interactions on ball motion and power draw in a laboratory-scale ball mill. The mill was simulated using *DEM* at different mill critical speeds and different filling levels. Totally, 165 simulation runs were conducted. Results indicated that at all mill filling levels, changing mill speed is of the greatest effect on power draw when the mill charge consists of 60% of small balls and 40% of big balls [39]. Kolahi et al. have investigated the effect of seven different types of liners on the performance of industrial scale ball mills. They suggested Osborn and Rib liners as suitable liners for the industrial ball mills. They showed that the type of liners, which is a function of the angularity of the lifters, the width of the lifters, and especially their height, strongly affects the performance of ball mills [40]. Jahani Chegeni and Kolahi, by introducing a couple of new parameters, that is to say, *HH* (Head Height) and *IZL* (Impact Zone Length) determined a proper range for the lifter number in pilot-scale ball mills using *DEM*. They concluded that the desirable range for the cuboid lifter number for them is between sixteen and thirty-two [41]. Recently, Safa and Aissat proposed helical lifters to advance the ball mill performance. *DEM* was used to predict the particle behavior, and conducted a comparative study on the influence of the lifter geometry and rotational speed of the mill on torque and power draw, as well as kinetic energy. The results show that using helical lifters has a more significant influence on the milling

efficiency, the torque, and the power draw of the ball mill [42].

In part 1 of this research work, five types of liners, i.e. Lorain, Osborn, Rib, cuboid, and Hi-lo are investigated. These liners all have separate lifters with the same volume. Their difference is in the width, height and type of lifter profile. First, all types of liners are simulated with four lifters using the Discrete Element Method (*DEM*). Then the lifter counts are increased four by four to fill the entire wall of the mill with lifters. Based on this, Lorain liner from 4 to 24 lifters, Rib liner from 4 to 40 lifters, Osborn liner from 4 to 120 lifters, and cuboid and Hi-lo liners from 4 to 64 lifters are simulated. For the first time, the Kinetic (*KE*) and Potential (*PE*) energies as well as the sum of these two energies (Total Energy) (*TE*) of all the balls have been obtained throughout the simulation time from zero to thirteen seconds and in each time step. Also their corresponding graphs for all five types of liners and all lifter numbers from four upwards are drawn, and compared in details. As previously mentioned, a good many of methods have been introduced by various researchers to calculate the energy consumption and power draw of ball mills such as the use of torque sensors, etc. However, the issue is that in none of the previous researches, the method and procedure of calculating the energy/power of the mills, whether by using *DEM* or by using other methods, has not been clearly and explicitly stated. In other words, researchers have only stated that the energy/power of a certain mill was calculated. But they have not mentioned anything about how to calculate it. Nonetheless, in the current research, *KE* and *PE* have been accurately calculated according to the mass, coordinates, height, and speed of all the balls at any time step according to $KE = 1/2mV^2$ and $PE = mgh$ formulas, where, *m* is the mass of the ball (kg), *V* is the speed of the ball (m/s), *g* is the acceleration of gravity (m/s^2), and *h* is the height of the ball from the bottom of the mill (m). First, *KE* and *PE* for a single ball are calculated. Then to calculate the *KE* and *PE* of all the balls, these values are added together to obtain the total *KE* and *PE*. Calculating the coordinates, height, and speed of all balls in all time steps and during the simulation time from zero to thirteen seconds for all liner types and

lifter count mentioned above is a very time-consuming process, and took about two years, which has been done for the first time by the authors of this article. It is worth mentioning that, given the *KE* and *PE* of all balls, the optimal lifter count can be obtained for each type of liner. Also in order to validate the simulation results, the power draw of an industrial operating ball mill (Meskavan ball mill) is obtained from the control room data. Then this value is compared with the *KE*, *PE*, and *TE* of all the balls obtained from *DEM* simulation, which showed a good agreement.

2. Ball Mill Configuration

In this research work, an industrial-scale ball mill with dimensions of 3.17 m × 5.70 m is investigated. Five types of liners, i.e. Lorain, Osborn, Rib, cuboid, and Hi-lo were installed inside the mill. These liners all have separate lifters with the same volume. Their difference is in the width, height, and type of lifter profile (Figure 1). Table 1 shows the exact geometric characteristics of the lifters used in this research work. First, all types of liners were simulated with four lifters using the Discrete Element Method (*DEM*). Then the lifter count was increased four by four to fill the entire wall of the mill with lifters. Based on this, Lorain liner from 4 to 24 lifters, Rib liner from 4 to 40 lifters, Osborn liner from 4 to 120 lifters, and cuboid and Hi-lo liners from 4 to 64 lifters were simulated. (Figures 2–6). In total, 78 simulation runs were performed in Part 1 of this research work.

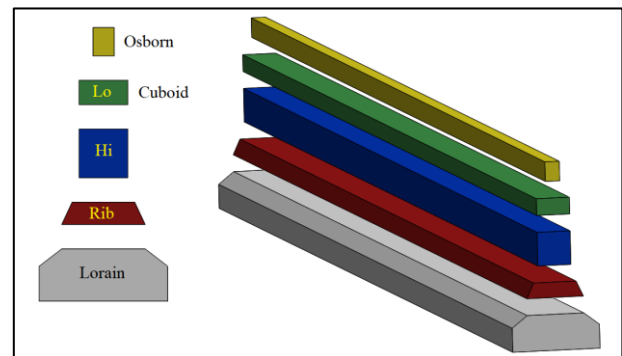


Figure 1. 2D profiles and 3D geometries of lifters used in five types of liners studied in this research work.

Table 1. Detailed geometric specifications of used lifters.

Liner type	Lifter large width (connected to the mill wall) (cm)	Lifter small width (where it hits the balls) (cm)	Lifter height (cm)	Lifter length (m)	2D geometry	
Lorain	36.50	24.30	15.44	5.70		
Rib	24.30	18.15	6.40	5.70		
Cuboid (Lo-lo)	14.00	14.00	7.00	5.70		
Hi-lo	Hi	14.00	14.00	14.00	5.70	
	lo	14.00	14.00	7.00	5.70	
Osborn	6.09	6.09	8.15	5.70		

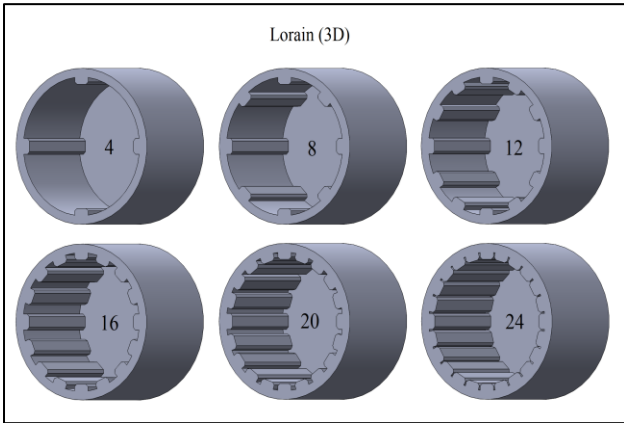


Figure 2. 3D geometries of industrial ball mills with Lorain liner from 4 to 24 lifters.

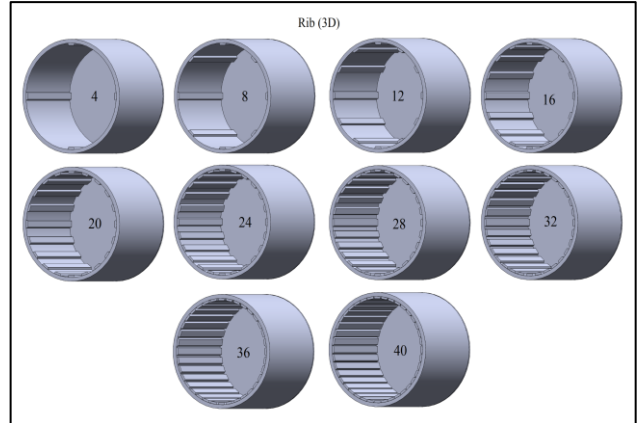


Figure 3. 3D geometries of industrial ball mills with Rib liner from 4 to 40 lifters.

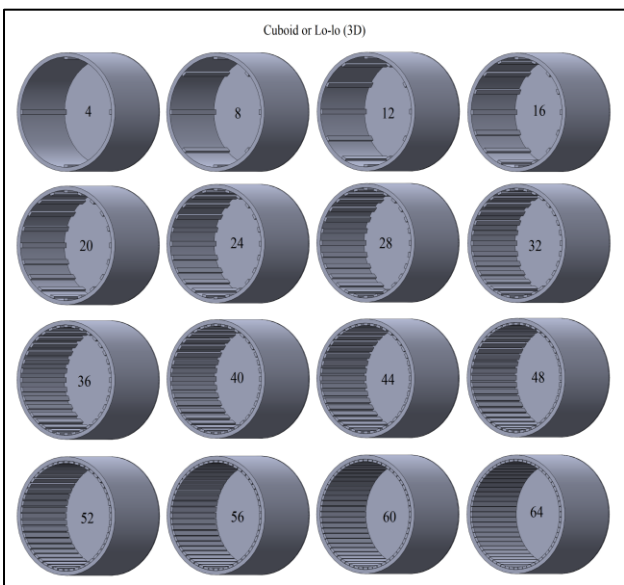


Figure 4. 3D geometries of industrial ball mills with the cuboid (Lo-lo) liner from 4 to 64 lifters.

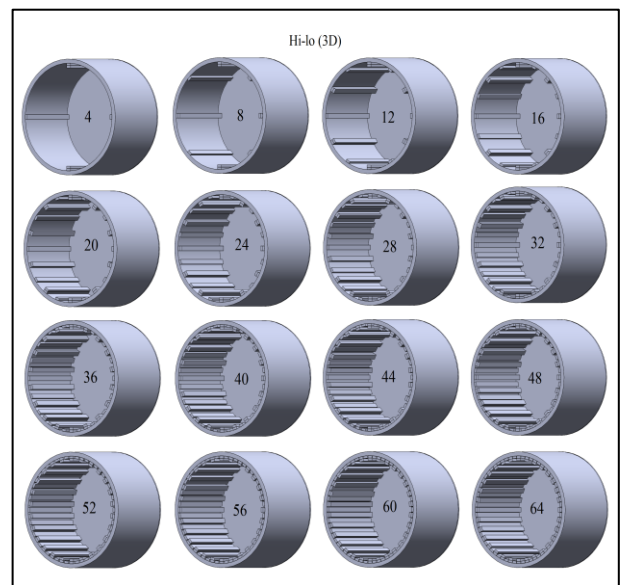


Figure 5. 3D geometries of industrial ball mills with Hi-lo liner from 4 to 64 lifters.

Detailed operating and geometric conditions, material properties, and calculations for these industrial scale ball mills are tabulated in Tables 2–4. It is worth noting that in this research work, all balls have the same diameter of 6 cm. The reason for keeping the ball diameter constant is to prevent the effect of changing their size on the *KE* and *PE* of all the balls. Optimizing the ball size distribution for all liners studied in this research is the subject of authors' future researches. In Table 4, the particle interaction distance (neighborhood), i.e. the distance that the particles exert a vertical and shear force on each other, is calculated as follows: One twentieth (5%) radius of the smallest particle

(30 mm). It is noteworthy to mention that the material of the balls and walls of the mills used in these simulations is stainless steel. The parameters used in Tables 3 and 4 such as ball density, ball sliding friction coefficient, ball rolling friction coefficient, Poisson ratio, Young's modulus, and ball restitution coefficient belong to stainless steel, and obtained from reputable internet websites. Table 5 shows the volume of a single lifter for the five types of liners investigated in this research. Table 6 demonstrates the useful internal volume of all mills after installation of different lifter count for the five types of liners studied here.

Table 2. Dimensions and velocities of the industrial-scale ball mill.

Industrial scale ball mill	Value
Mill inside length (m)	5.70
Mill inside diameter (m)	3.17
Inside volume of no lifter mill (m ³)	44.98661 = 44.99
Critical Speed (CS) (rpm)	23.99
Mill rotation speed (80% of CS) (rpm)	19.19
Mill rotation direction	Clockwise

Table 3. Calculations and specifications of DEM balls.

Ball diameter (cm)	6
Volume of a single ball (m ³)	$1.13097 \times 10^{-4} = 1.13 \times 10^{-4}$
Filling of mill ball charge (%)	40%
Volume of all balls (m ³)	$40\% / 2 \times 44.98661 = 8.99732 = 9.00$
Number of balls in simulation	$8.99732 / 1.13097 \times 10^{-4} = 79553$
Ball density (kg/m ³)	8050
Total mass of balls (kg)	$8050 \times 8.99732 = 72428.44104 = 72428.44$

Table 4. Parameters of DEM simulations.

DEM model details	Value
DEM spring constant (kg/m)	10^6
Ball sliding friction coefficient	0.5
Ball rolling friction coefficient	0.0015
Poisons ratio	0.285
Young's modulus (N/m ²)	1×10^9
Ball restitution coefficient	0.817
Time step (s)	$0.0001 = 10^{-4}$
Period of 80% CS	$60 / 19.19 = 3.12681$
Particle interaction distance (m)	$5\% \times 30 \text{ mm} = 15 \times 10^{-4}$

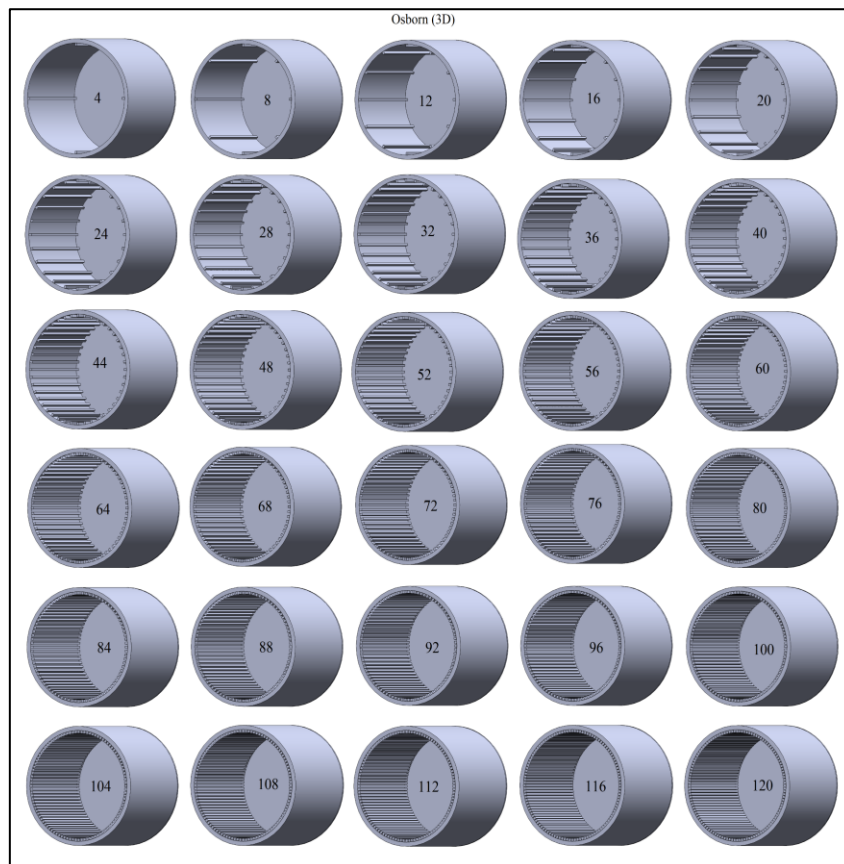


Figure 6. 3D geometries of industrial ball mills with Osborn liner from 4 to 120 lifters.

Table 5. Volume of a single lifter for five liner types studied here.

Lifter count	Volume of a single lifter (m ³)														
	4	8	12	16	20	24	28	32	36	40	44	48	52	56	60
Lorain	0.1294														
Rib	0.0774														
Cuboid	0.0559														
Liner type	Hi	0.1117													
	Lo	0.0559													
	Ave	0.0838													
Osborn	0.0283														

lifter count	Volume of a single lifter (m ³)													
	68	72	76	80	84	88	92	96	100	104	108	112	116	120
Liner type	Osborn	0.0283												

Table 6. Useful internal volume of all mills after installation of different lifter counts.

lifter count	Mill inside volume (m ³)															
	4	8	12	16	20	24	28	32	36	40	44	48	52	56	60	64
Liner type	Lorain	43.78	42.57	41.35	40.14	38.93	37.72	-	-	-	-	-	-	-	-	-
	Rib	44.68	44.37	44.06	43.75	43.44	43.13	42.82	42.51	42.20	41.89	-	-	-	-	-
	Cuboid	44.76	44.54	44.32	44.09	43.87	43.65	43.42	43.20	42.98	42.75	42.53	42.31	42.08	41.86	41.64
	Hi-lo	44.65	44.32	43.98	43.65	43.31	42.98	42.64	42.31	41.97	41.64	41.30	40.96	40.63	40.29	39.96
	Osborn	44.87	44.76	44.65	44.53	44.42	44.31	44.19	44.08	43.97	43.85	43.74	43.63	43.52	43.40	43.29

lifter count	Mill inside volume (m ³)														
	68	72	76	80	84	88	92	96	100	104	108	112	116	120	
Liner type	Osborn	43.06	42.95	42.84	42.72	42.61	42.50	42.38	42.27	42.16	42.04	41.93	41.82	41.70	41.59

3. Results and Discussion

3.1. DEM simulations of industrial ball mills

Figure 7 illustrates DEM simulation legend for all simulations conducted throughout this research work. Blue balls have the lowest speed, while red balls have the highest speed, with a speed of about 4 m/s. The reason for the separate display of the legend is to preserve the symmetry in the simulation images, and to reduce the size of the figures. All the snapshots for all the liners studied in this research work were taken within 5 seconds after the mill came to its steady state. In all the simulations, the duration of the simulation was 13 seconds, and for most of the liners, the mill reached a steady state after 3 to 5 seconds. Therefore, for comparison, all snapshots were taken at 5 seconds.

Figure 8 demonstrates three-dimensional DEM simulation snapshots (front view) of industrial ball mills with Lorain liner from 4 to 24 lifters. Lorain liner lifters have the widest width among all the liners studied in this research work (36.5 cm), and it is not possible to install more than 24 lifters inside the mill shell (for example, 28 lifters; however, it may be possible to install 25 or 26 lifters inside the mill shell. But since the lifter count has been increased four by four, their maximum number is 24. As it can be seen, in all modes (4 to 24 lifters), this liner has the ability to create cascading and cataracting motions. In the 4-lifter

mode, the distance between the lifters is very large, which causes the loss of cataracting motions at some moments in the mill. In the 24-lifter mode, the distance between the lifters is very small, which reduces the volume of the mill from 44.99 m³ to 37.72 m³. It means 83.85% of the initial volume of the no-lifter mill. In this case, the balls cannot enter the space between the two lifters, and the volume of the mill is greatly reduced. Therefore, in terms of volume, the 24-lifter mode is not recommended for the Lorain liner.

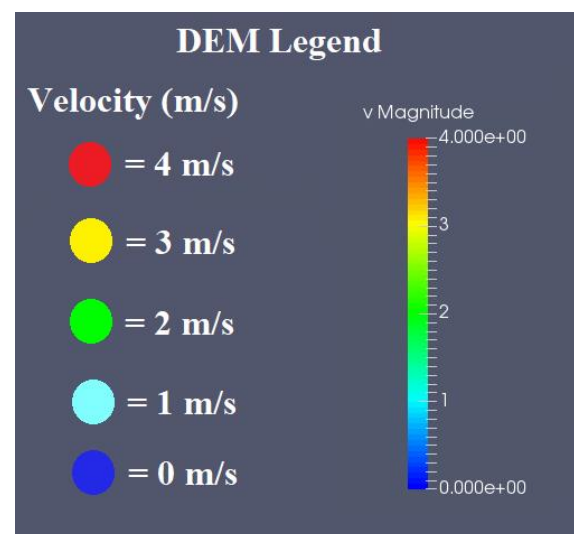


Figure 7. DEM simulation legend for all simulations.

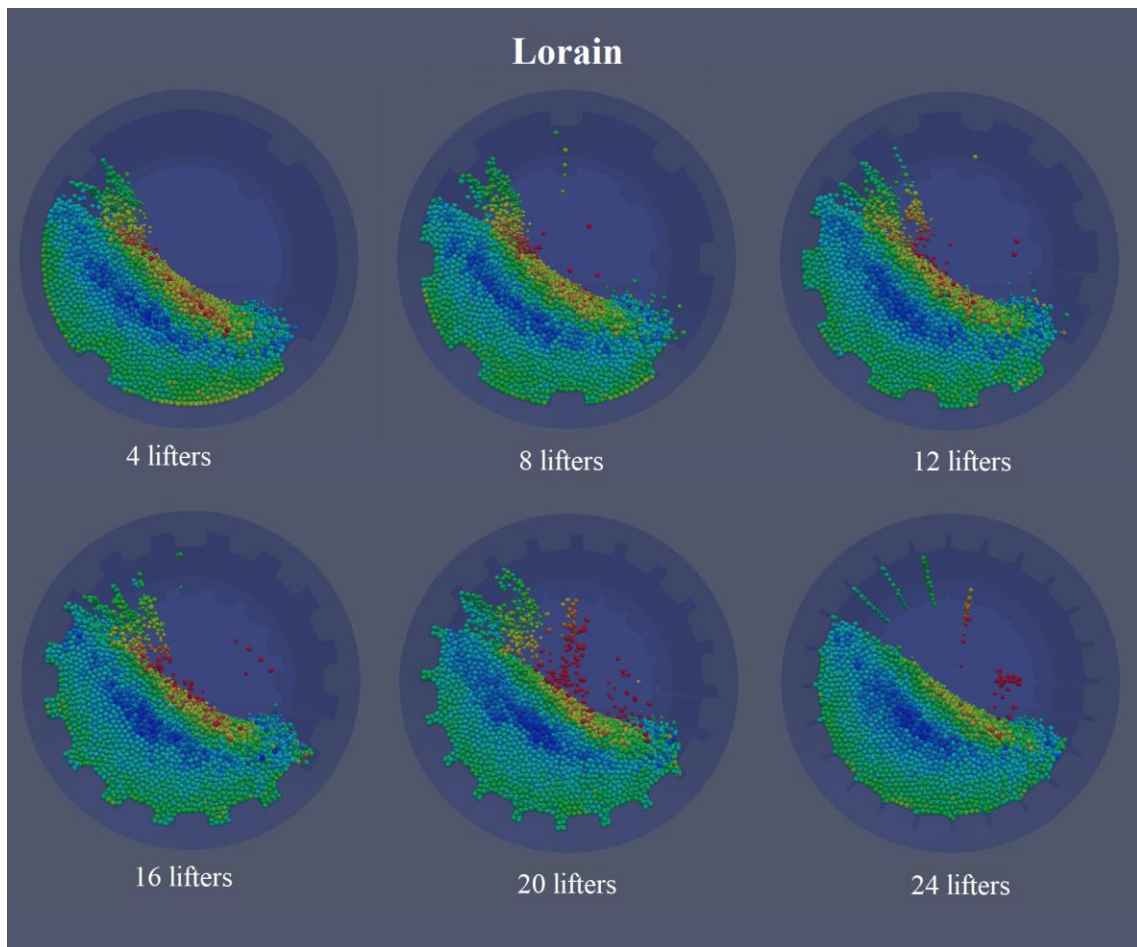


Figure 8. 3D DEM simulation snapshots (front view) of industrial ball mills with Lorain liner from 4 to 24 lifters.

Figure 9 demonstrates three-dimensional DEM simulation snapshots (front view) of industrial ball mills with Rib liner from 4 to 40 lifters. After Lorain liner, Rib liner has the widest width (24.30 cm) among the liners examined in this research work. Therefore, it is not possible to install more than 40 lifters inside the mill shell. On the contrary, Rib liner has the lowest height (6.40 cm) among the liners examined in this research work. Like Lorain liner, Rib liner also has the ability to create cascading and cataracting motions in all modes (from 4 to 40 lifters). In the 4-lifter and 8-lifter modes, due to the small lifter count, cataracting motions are not observed in all simulation moments. In the modes of 24, 28, and 32 lifters, the performance of this liner seems optimal. The reason for that is the proper distance, and sufficient lifter count. However, in the 36-lifter and 40-lifter modes, the size of the balls is almost equal to the distance between the lifters, and the balls are trapped in this distance, which causes the mill's performance to be out of optimal mode. Due to the small distance between the lifters, in these two cases, a large number of balls stick to the wall of the mill, and do not participate in the grinding

mechanism. After installing the Rib liner in the 40-lifter mode, the useful volume of the mill has decreased from 44.99 m³ to 41.89 m³. That is, it has decreased by about 7%, which is much less than Lorain liner in the 24-lifter mode (about 16%). In general, considering the proper performance of Lorain and Rib liners in all modes, it can be concluded that the trapezoidal profile is suitable for industrial ball mill liners.

Figure 10 demonstrates three-dimensional DEM simulation snapshots (front view) of industrial ball mills with cuboid or Lo-lo liner from 4 to 64 lifters. In the 4- to 44-lifter modes, cascading and cataracting motions are observed in all mills. In the 40-lifter mode, the distance between the lifters is almost twice the diameter of the balls. For this reason, a good many of balls are trapped in pairs in this distance, and do not participate in the grinding. Therefore, the mill is far from its optimal state. This increases the PE of the balls (Figure 15e), and a small hump is observed in the diagram. The best performance of this liner happened in the 44-lifter mode, where cataracting motions were created alternately and continuously, and also appropriate shoulder and toe points were

created. But in the 48-lifter mode, because the distance between the lifters is almost the same as the diameter of the balls, all the balls are trapped in this distance, and there is practically no impact mechanism in this case, and grinding is done only based on the abrasion mechanism, which must be taken into account in the design of liners. The way to identify is that a sudden increase in the *PE* of the balls is observed (Figure 15e), and a big hump is seen in this graph. In 56 to 64-lifter modes, the

performance of the mill is significantly weakened, so that in these modes, the mill becomes a lifter-less mill with a smaller volume. Therefore, an excessive increase in the lifter count will destroy their efficiency. In the 64-lifter mode, the useful volume of the mill has decreased from 44.99 m³ to 41.41 m³. It means that the volume has decreased by about 8%, which makes their use completely uneconomical due to the purchase and installation costs of lifters.

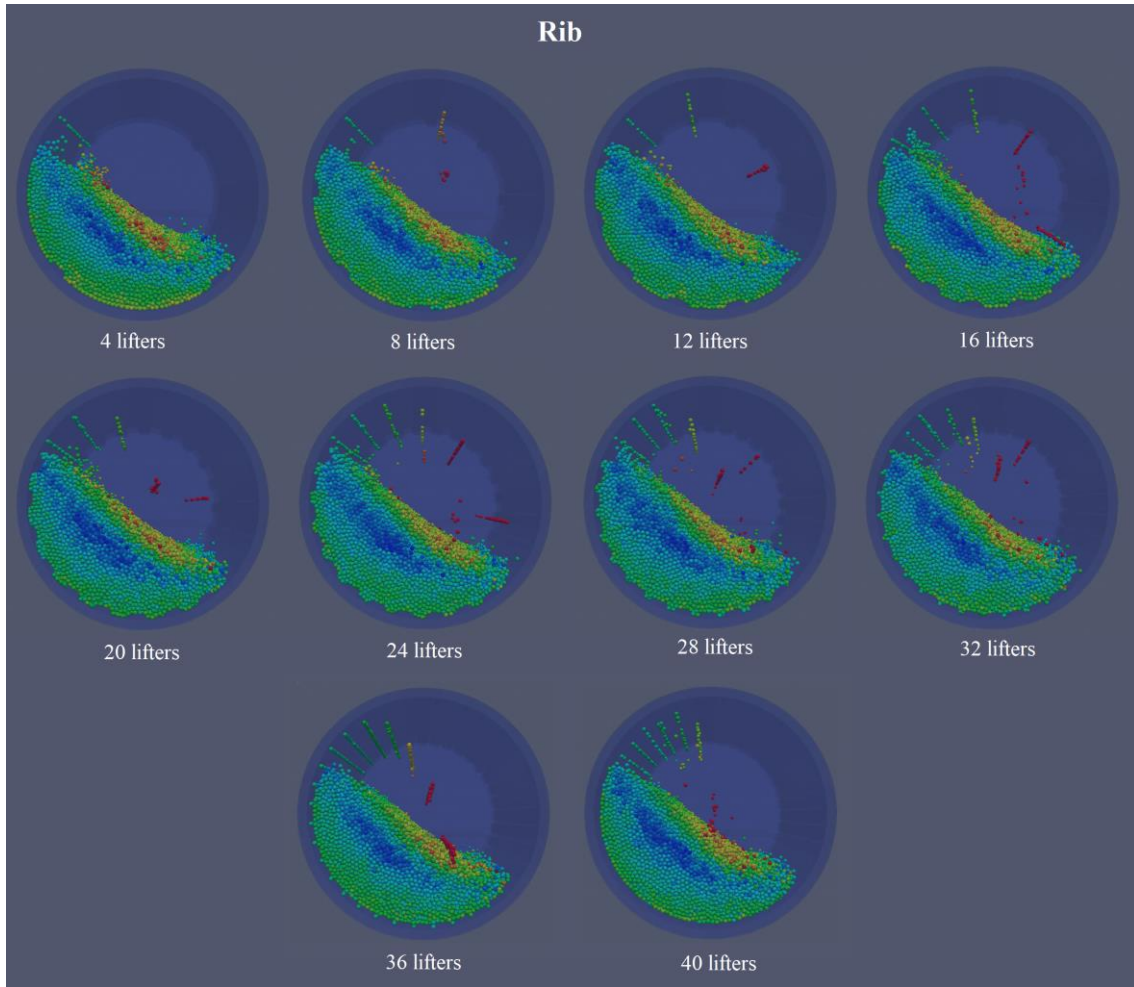


Figure 9. 3D DEM simulation snapshots (front view) of industrial ball mills with Rib liner from 4 to 40 lifters.

Figure 11 demonstrates three-dimensional DEM simulation snapshots (front view) of industrial ball mills with Hi-lo liner from 4 to 64 lifters. By doubling the height of half of the lifters of the cuboid (Lo-lo) liner, as one in between, i.e. increasing their height from 7 cm to 14 cm, this liner turns into a Hi-lo liner. Unlike the Lo-lo liner, in the Hi-lo liner, in all modes (4 to 64 lifters), cascading and cataracting motions are observed, and its 64-lifter mode is similar to the 32-lifter mode of the Lo-lo liner, but with a smaller volume (39.62 m³ against 43.20 m³). Therefore, the main advantage of installing Hi-lo liners in the mill is

that in no case, the mill does not perform like a lifter-less mill. The mills shows good performance in 16 to 52-lifter modes, which this range is much wider than the Lo-lo liner. The best performance of the mill is related to the 36 and 44-lifter modes, where cataract motions are created alternately and continuously. They also have appropriate shoulder and toe points. In the 40-lifter mode, because the distance between the lifters is about twice the diameter of the balls, the balls are trapped in pairs at these distances, and are stuck to the mill wall, and practically, do not participate in grinding. As a result, the operation of the mill has been moved

away from the optimal state. Also in Figure 16e, in the 40-lifter mode, a hump can be seen in the graph, which indicates the increase in the *PE* of the balls in this mode. In the 48-lifter mode, because the distance between the lifters is almost equal to the diameter of the balls, a great many of balls are trapped individually in these distances, and practically do not participate in grinding. But the difference here with the Lo-lo liner is that some of

the balls have managed to get out of these distances due to the height difference between the lifters, and can help with optimal grinding. Once more, in Figure 16e, a large hump can be seen for the 48-lifter liner, which indicates a sudden increase in the *PE* of the balls. In the 52-lifter mode, there is a better grinding than the similar mode in the Lo-lo liner.

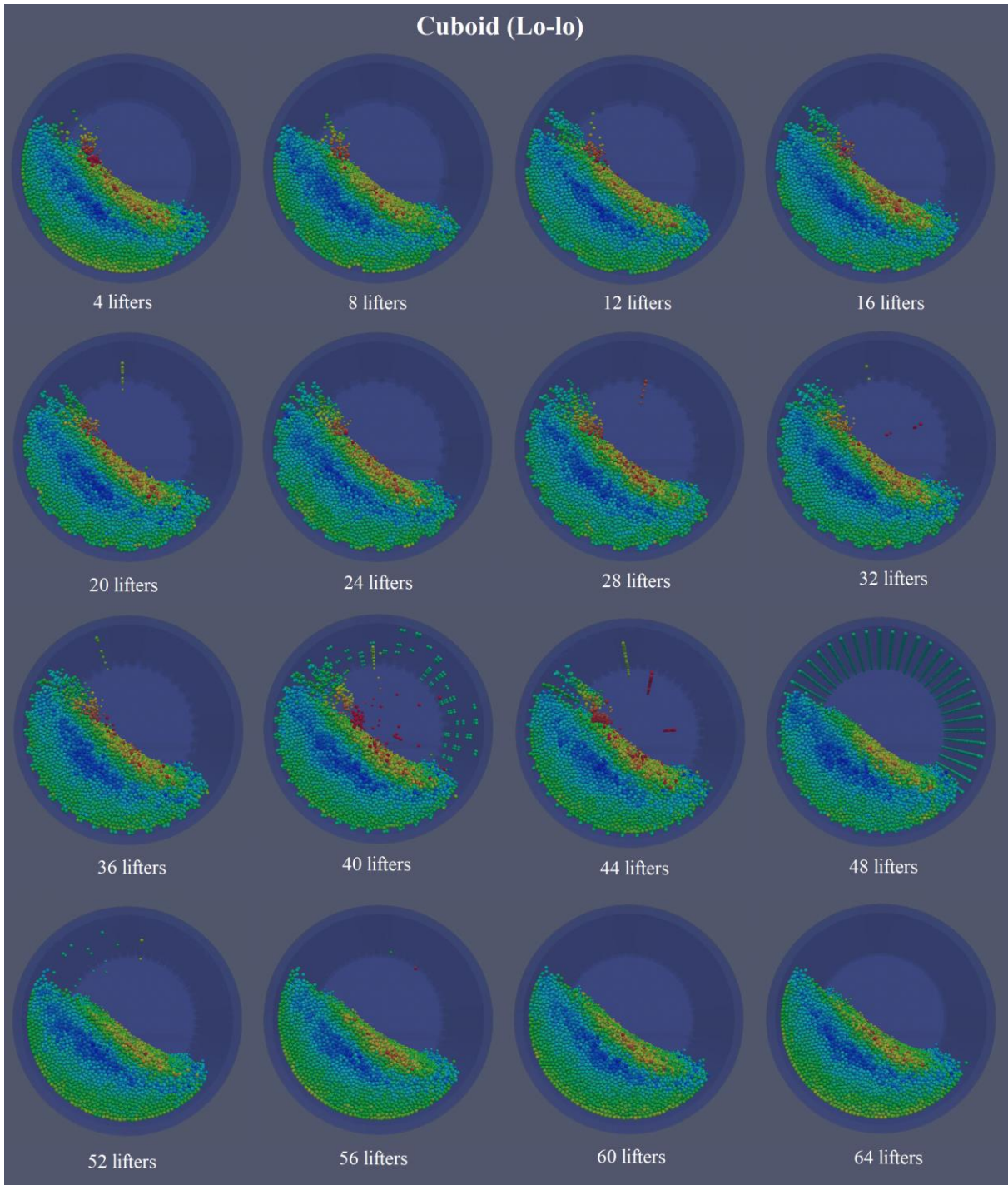


Figure 10. 3D DEM simulation snapshots (front view) of industrial ball mills with cuboid (Lo-lo) liner from 4 to 64 lifters.

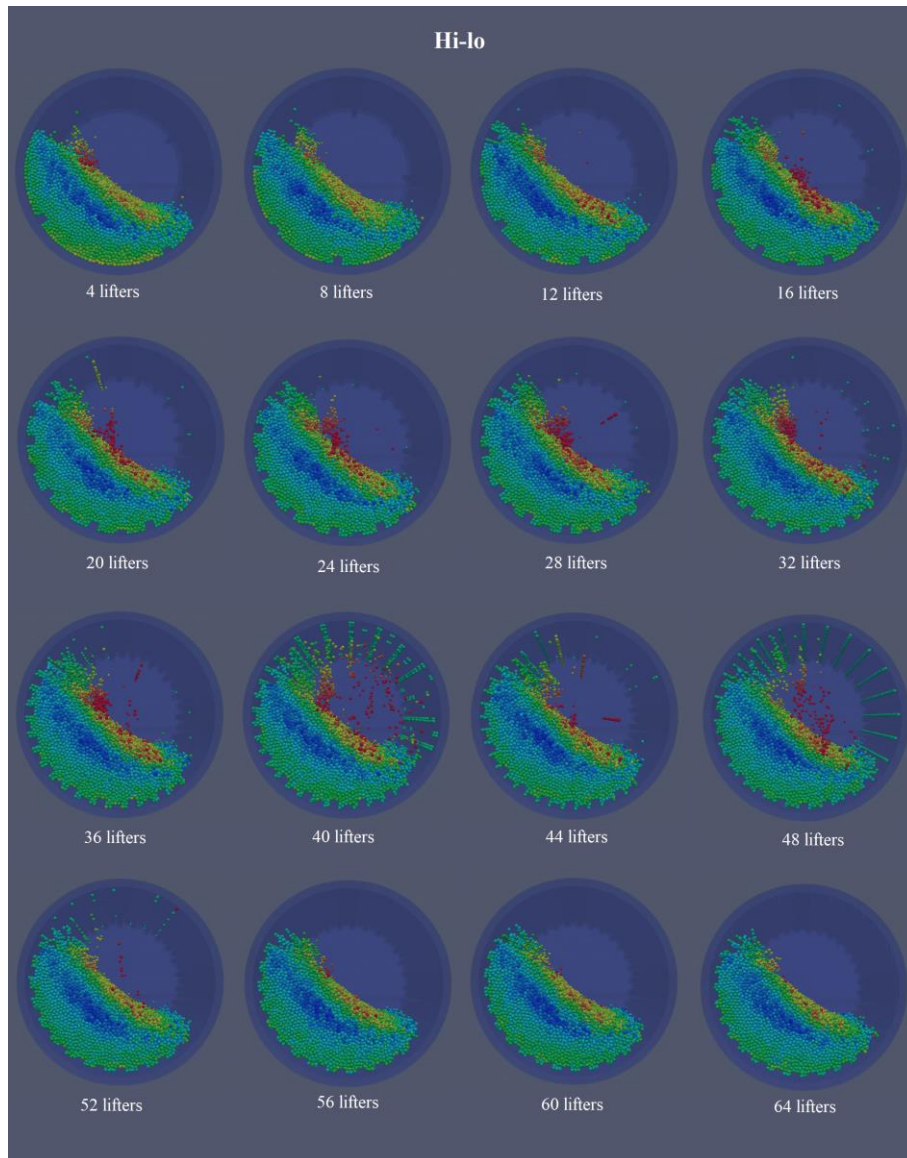


Figure 11. 3D DEM simulation snapshots (front view) of industrial ball mills with Hi-lo liner from 4 to 64 lifters.

Figure 12 demonstrates three-dimensional DEM simulation snapshots (front view) of industrial ball mills with Osborn liner from 4 to 120 lifters. Osborn liner has the smallest width among the liners studied in this research work (6.09 cm). Consequently, compared to other liners, more lifters of this type can be installed in the wall of the mill (120 lifters). In the 4 to 92-lifter modes, cascading and cataracting motions are observed in all mills. But from 96 lifters onwards, these motions gradually disappear, so that in 100 to 120-lifters modes, cascading motions are practically not observed, and the mills work like a lifter-less mill and with a smaller volume. In the 20 to 88-lifter modes, the performance of the mills is favorable. The best performances are related to the modes of 64, 68, 72 and 76-lifters, and this range can be introduced as the optimal performance range of the Osborn liner. In this range, cataracting motions are

clearly visible intermittently and continuously. Also suitable shoulder and toe points are created for the balls. In the 60- lifter mode, the distance of the lifters is almost twice the diameter of the balls, and the balls are trapped in pairs in these distances, which weaken the grinding performance. This has caused a sudden increase in the *PE* of the balls (Figure 17e). As can be observed, a big hump can be seen in the 60-lifter mode in the chart. One more time, in the 80-lifter mode, the distance of the lifters is almost equal to the diameter of the balls, and the balls are trapped individually in these distances, which weaken the performance of the mill. This issue has afresh caused a sudden increase in the *PE* of the balls (Figure 17e). As can be seen, the second big hump is also clearly visible in the 80-lifter mode in the chart. In the 84 to 96-lifter modes, the reason for the balls to rise is because they get stuck on the edge of the lifters. As the lifter

count increases, the number of lifted balls decreases, and finally reaches zero in the 100-lifter mode. In general, unlike the Hi-lo liner, in the Osborn liner, similar to the Lo-lo liner, due to the

same height of all the lifters, there is a possibility of losing the effect of the lifters and reducing the mill volume, which should be considered by the liner designers.

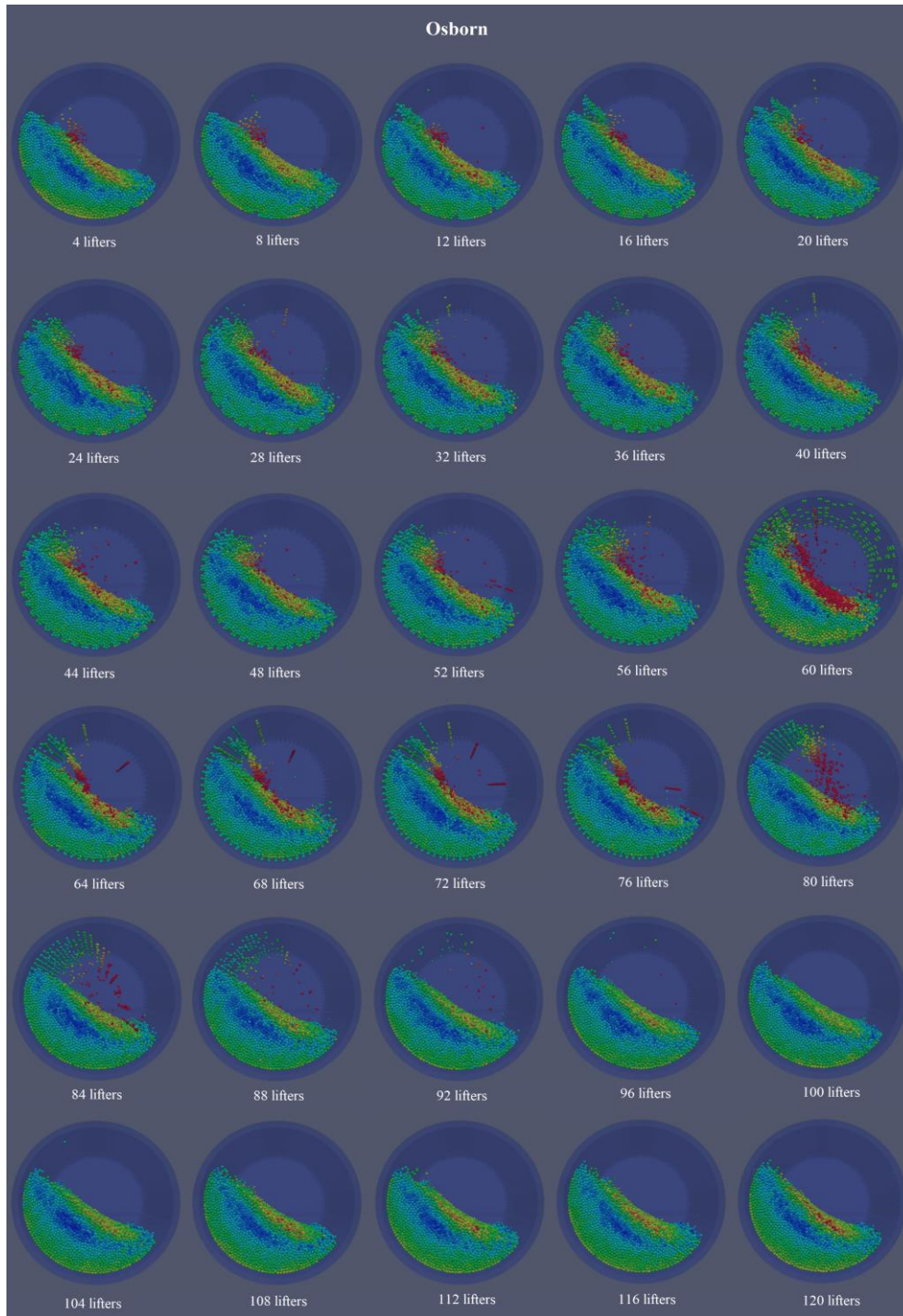


Figure 12. 3D DEM simulation snapshots (front view) of industrial ball mills with Osborn liner from 4 to 120 lifters.

3.2. Calculation of KE, PE, and TE of the balls for the studied liners.

In this research work, for the first time, KE and PE as well as the sum of these two energies (TE =

KE + PE) of all the balls are calculated, and compared throughout the simulation time from zero to thirteen seconds for all the liner types and lifter counts mentioned above. This task, i.e. calculating the KE and PE at each time step, was

very laborious, and lasted for about two years. Also their corresponding graphs for all five types of liners and all lifter numbers from four upwards are drawn and compared in detail (Figs 14–20). The KE , PE , and TE have been accurately calculated according to the mass, coordinates, height, and speed of all the balls at any time step according to $KE = 1/2mV^2$, $PE = mgh$, and $TE = KE + PE$ formulas, where m is the mass of the ball (kg), V is the speed of the ball (m/s), g is the acceleration of gravity (m/s^2), and h is the height of the ball from the bottom of the mill (m). First, the KE_i and PE_i for a single ball (ball i) were calculated (Equations 1 and 2), where, m_i is the mass of the ball i (kg), V_i is the speed of the ball i (m/s), and h_i is the height of the ball i from the bottom of the mill (m). Then to calculate the KE and PE of all the balls, these values were added together to obtain the KE and PE of all particles (Equations 3 and 4).

$$KE_i = \frac{1}{2}m_iV_i^2 \tag{1}$$

$$i = 1, 2, \dots, 79553$$

$$PE_i = m_i gh_i \tag{2}$$

$$i = 1, 2, \dots, 79553$$

$$KE = \sum_{i=1}^{79553} KE_i \tag{3}$$

$$PE = \sum_{i=1}^{79553} PE_i \tag{4}$$

After the mill starts to rotate, first the KE and PE of the balls increase greatly. After some time since the mill started working, these energies get to their minimum value. Then in most mills, they come to a relative steady state in about 3 seconds, which we called steady state 1 (here, 3-13s). But in some mills, it takes about 5 seconds to get to the steady state, which we called steady state 2 (here, 5-13s). To ensure that all mills studied in this research work, with different types of liners and different numbers of lifters, have reached steady state, this final steady state is defined. Therefore, the graphs related to KE and PE are drawn in three states: 0 to 13 s (total simulation time), 3 to 13 s (after steady state 1), and 5 to 13 s (after steady state 2).

Figure 13a demonstrates the values of KE for Lorain liner from 4 to 24 lifters during simulation time from 0 to 13s. As can be seen, in about 1.5 to 2 s, the KE of the balls has reached its maximum value in all lifters. In about 2.5 to 3s, the KE of the

balls has come to its minimum value in all lifters. After coming to the steady state (5-13s), the 4-lifter liner has created the highest amount of KE for the balls (about 67 kJ). By increasing the lifter count from 4 to 24, the value of KE of the balls has decreased (about 50 kJ). Also the amount of KE fluctuations has decreased. In the 4-lifter mode, there are many fluctuations in the value of KE . The reason is the low lifter count in this situation. After the lifter hits the balls, their KE increases. But in places where there is no lifter, their KE is reduced. In the 20 and 24-lifter modes, the amount of KE fluctuations has reached its lowest value, which indicates the appropriate and sufficient lifter count in these two modes. Therefore, it can be concluded that when the KE of the balls has less fluctuations, the number of mill lifters is suitable. On the contrary, when the fluctuations of the KE of the balls are high; it indicates that the lifter count is not enough and the motion of the balls in the mill is not uniform and stable. Figure 13b demonstrates the values of PE for Lorain liner from 4 to 24 lifters during simulation time from 0 to 13s. This figure shows that the PE of the balls, like their KE , has come to its maximum value in about 1.5 s; then it has reached its minimum value in about 2.5s. After getting into a steady state (5-13s), it can be seen that with the increase in the lifter count from 4 to 24; the PE of the balls has increased (it has come to 695 kJ from about 610 kJ). Once more, the amount of PE fluctuations in the 4-lifter mode is significant compared to other modes, which indicates that the lifter count is not enough. In the 20 and 24-lifter modes, the value of PE of the balls is almost constant, which indicates the appropriate lifter count. Therefore, from the fluctuations of the PE of the balls, it is possible to find out whether the lifter count is sufficient or not. By comparing the values of the KE of the balls (Figure 13a), and their PE (Figure 13b); it can be concluded that the value of PE of the balls is much higher than the value of their KE . For example, in the 20-lifter mode, the KE of the balls is about 55 kJ, while their PE is about 675 kJ (more than 12 times). This shows that the PE of the balls is more important than their KE and lifters, which can raise the balls to a higher height are more suitable. This figure also shows the values of TE for Lorain liner from 4 to 24 lifters during simulation time from 0 to 13 s (Figure 13c). This figure indicates that the TE of the balls also shows a behavior similar to their PE . In other words, the role of the PE of the balls in the TE is much stronger than the role of their KE . One more time, by increasing the lifter count from 4 to 24, the TE of the balls has increased. Also this figure

shows the average of *KE* (d), the average of *PE* (e), and the average of *TE* (f) of balls for Lorain liner from 4 to 24 lifters. Figure 13d shows that the average *KE* of the balls in the 4-lifter mode after the steady state (5-13s) has decreased from about 66 kJ to about 51 kJ in the 24-lifter mode. Therefore, there is an inverse relationship between the *KE* of the balls and the number of mill lifters in the Lorain liner. Figure 13e shows that the average *PE* of the balls after the steady state has reached

from about 610 kJ in the 4-lifter mode to about 693 kJ in the 24-lifter mode. Therefore, there is a direct relationship between the *PE* of the balls and the number of mill lifters in the Lorain liner. Also Figure 13f shows that the average *TE* of the balls after the steady state has increased from about 675 kJ in the 4-lifter mode to about 745 kJ in the 24-lifter mode. Therefore, there is also a direct relationship between the *TE* of the balls and the number of mill lifters in the Lorain liner.

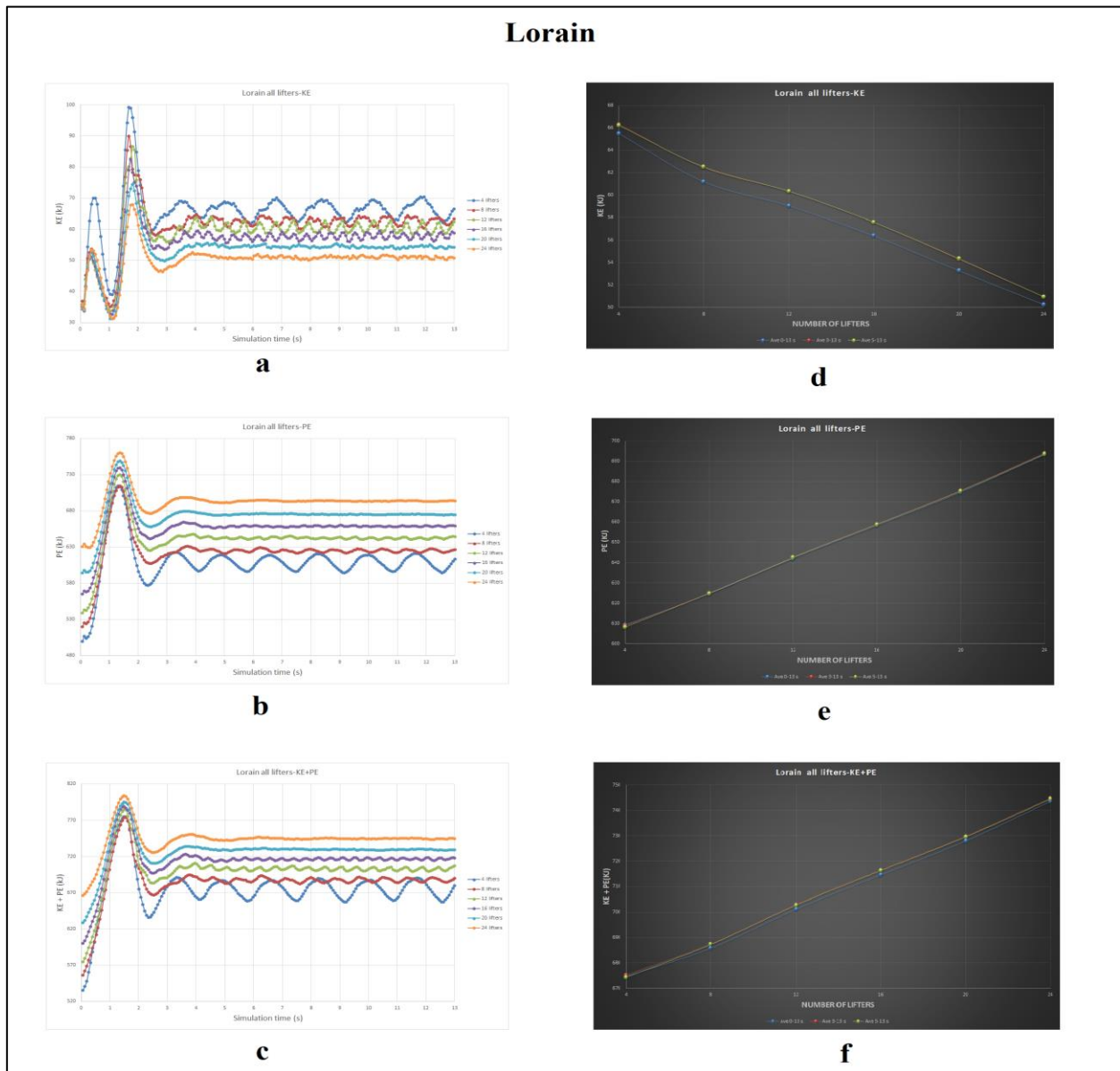


Figure 13. Values of a) *KE*, b) *PE*, c) *TE*, d) the average of *KE*, e) the average of *PE* and f) the average of *TE* of balls for the Lorain liner from 4 to 24 lifters.

Figure 14 demonstrates the values of *KE*, *PE*, *TE* of balls, and their averages for the Rib liner from 4 to 40 lifters during simulation time (0 to 13s). In Figure 14a, after starting the mill, the *KE* of the balls first increased in 0.5s for all modes (4-lifter to 40-lifter). Then it came to its minimum in

about 1.2s. One more time, it has gotten into its maximum in about 1.8 s, and has reached an almost steady state in about 3.5 s. In the 4-lifter mode, the amount of fluctuations in the *KE* of the balls is high in the Rib liner, similar to the Lorain liner, which is due to the small lifter count in this mode. Also in

the 8-lifter mode, the amount of fluctuations is significant compared to other modes. But in other modes from 12 to 40 lifters, the amount of fluctuations of the *KE* of the balls is insignificant, which indicates that the lifter count in these modes is sufficient. In Figure 14b, after starting the mill, the *PE* of the balls in all modes from 4 to 40 lifters has come to its maximum in about 1.3s. Then it got to its minimum in about 2.3s. This figure also shows that the *PE* of the balls in the Rib liner; unlike the Lorain liner, has an oscillating (sinusoidal) state, and continuously increases and decreases, and even after 13 seconds; it does not reach a steady state. The reason can be attributed to the low height of the Rib liner. It can be said that if the height of the liner is less than a certain limit, it will take longer than normal for the mill to get to a steady state. In general, mill performance can be improved by increasing Rib liner height. Also in Figure 14c, after starting the mill, the *TE* of the balls comes to its maximum in about 1.5s, and gets to its minimum in about 2.5s. This figure shows that the *TE* of the balls, like their *PE*, has an oscillating and sinusoidal state, and does not reach a steady state even after the completion of the simulation time (13s). Consequently, it is possible to decide whether or not the height of the lifters is appropriate based on the information related to the fluctuations of *PE* and *TE*. Figure 14d shows the average values of the *KE* of the balls. As can be seen, in the 4-lifter mode, the amount of *KE* of the balls is about 60 kJ, which has decreased to about 50 kJ with the increase of the lifter count to 32 lifters. But surprisingly, in the 36- and 40-lifter modes, the value of *KE* of the balls has increased again!, which can indicate that the mill is moving away from the steady state. In general, with the increase in the lifter count in the Rib liner similar to the Lorain liner; the *KE* of the balls has decreased, and there is an inverse relationship between them. Figure 14e shows that with the increase in the lifter count from 4 to 40, the *PE* of the balls increases. In the 4-lifter mode, the *PE* of the balls is about 597 kJ, which has come to about 634 kJ in the 40-lifter mode. In general, as the lifter count increases, because they raise the balls to a higher height, the *PE* of the balls increases, and there is a direct relationship between the lifter count and the *PE* of the balls. Figure 14f shows that the *TE* of the balls also increases with the increase in the lifter count, similar to their *PE*. Only in the 32-lifter mode, the value of *TE* has been almost constant compared to the 28-lifter mode. In general, it can be said that the *PE* of the balls has a greater contribution to their *TE* than the *KE*. For

example, in the 28-lifter mode, the *KE* of the balls is about 53 kJ, their *PE* is about 621 kJ, and their *TE* is about 674 kJ, that is, about 8% of the *TE* of the balls is related to their *KE* and the other 92% is related to their *PE*. Therefore, the role of the *PE* of the balls is much stronger than their *KE*, and the *PE* should be the basis of the analysis.

Figure 15 demonstrates the values of *KE*, *PE*, *TE* of balls, and their averages for cuboid (Lo-lo) liner from 4 to 64 lifters during simulation time from 0 to 13s. In Figure 15a, after starting the mill, in about 0.5 seconds, a sharp increase in the *KE* of the balls can be seen for all the lifter count (from 4 to 64). Then in about 1.2 s, the *KE* of the balls gets to its minimum. Then around 1.7s, it comes to its second maximum one more time. Finally, after 3 seconds, the amount of fluctuations in the *KE* of the balls decreases, and reaches a relatively steady state. The value of *KE* fluctuations in the 4-lifter mode is higher than other modes, which indicates the unsteady state of the mill in this mode, and indicates the low lifter count. In Figure 15b, after starting the mill, in about 1.2s, the value of *PE* of the balls gets to its maximum in all modes. Then it comes to its minimum in about 2.3s, and reaches a relatively steady state in about 3.5s. In some modes such as the 4-lifter mode, as well as the 52, 56, 60, and 64-lifter modes, large fluctuations in the *PE* of the balls can be observed, which is due to the low lifter count (in the 4-lifter mode) or the excessive lifter count (in the 52-64 lifter modes), and as a result, their ineffectiveness. In other words, whenever there are large fluctuations in the *PE* of the balls, it indicates the unfavorable performance of the mill and its inappropriate lifter count. The *TE* of the balls (Figure 15c) has a completely similar behavior to their *PE*. In Figure 15d; with the increase in the lifter count from 4 to 24, the *KE* of the balls has decreased from about 59.8 kJ to about 53.2 kJ. However, in the 28-lifter mode, an increase in the *KE* of the balls is observed anew. From 28-lifter to 36-lifter, the *KE* of the balls has decreased once more. Then from 36-lifter mode to 44-lifter mode, one more time increasing the *KE* of the balls can be seen. From 48-lifter to 52-lifter, the *KE* of the balls decreases afresh, and reaches about 50 kJ for the 52-lifter mode. After that, the *KE* increases anew up to the 60-lifter mode. In general, the *KE* of the balls in the Cuboid (Lo-lo) liner fluctuates around 10 kJ and does not follow a special rule, and for this type of liner, the *KE* of the balls cannot be used as the basis for deciding on the optimal lifter count. In Figure 15e; with the increase in the lifter count from 4 to 36, the *PE* of the balls has increased. Yet, in the 40-lifter mode,

a small hump can be seen in the graph, and the PE of the balls is almost equal to the 44-lifter mode. As mentioned before, and can be seen in Figure 10, the reason for this is that the balls are stuck in pairs in the space between the two lifters. In the 48-lifter mode, a sudden and significant increase in the PE of the balls can be seen (hump 2). One more time, according to the previous explanations in Figure 10, since in the 48-lifter mode, the distance between the lifters is almost equal to the diameter of the balls, a significant number of balls are individually trapped in this space, and they are attached to the wall of the mill, and do not participate in grinding. Hence, when observing a sudden jump in the PE diagram of the balls, their adhesion to the wall of the mill should be checked and this issue should be avoided. In the 52 to 64-lifter modes, an increase in the PE of the balls is observed once more. Nonetheless, according to Figure 10, cascade and cataract motions are not created in these cases. Therefore, the PE of the balls to some extent can help to choose the optimal lifter count. As such choosing the optimal lifter count should be done, considering the creation of cataracting motions; the creation of appropriate shoulder and toe points, and the PE of the balls simultaneously. Considering the above factors, the optimal lifter count for the cuboid liner in the ball mill studied in this research is 44. In Figure 15f, a similar trend of PE can be observed for the TE of the balls.

Figure 16 demonstrates the values of KE , PE , TE of balls, and their averages for Hi-lo liner from 4 to 64 lifters during simulation time from 0 to 13s. In Figure 16a, after starting the mill, the KE of the balls comes to its first maximum in about 0.4 s for all modes from 4 to 64 lifters. Then it gets to its lowest value in about 1.2s. Once more, it comes to its second maximum in about 1.8s, and around 4s, the amount of fluctuations in the KE of the balls decreases and a relative steady state is created for all the lifter count. In the 4-lifter mode, the amount of KE fluctuations is higher than in other modes, which indicates the low lifter count in this mode. In Figure 16b, after starting the mill, in about 1.3s, the PE of the balls reaches its maximum for all modes from 4 to 64 lifters. Then it gets to its minimum in about 2.5s, and comes to a relative steady state after 3s. The amount of fluctuations in the PE of the balls in the 4-lifter mode is higher than in other modes, which again confirms the low lifter count in this mode. In other modes, from 8 to 64 lifters, the curves have a sinusoidal state, which is due to the decrease in the height of the lifters in

the Lo mode and their increase in Hi mode. In other words, when the balls are affected by Lo lifters, their PE increases less, and when they are affected by Hi lifters, their PE increases more. The TE of the balls (Figure 16c) has a completely similar trend to their PE . In Figure 16d, it can be seen that with the increase in the lifter count from 4 to 64, the KE of the balls has decreased in almost all cases and has reached from about 62 kJ in the 4-lifter mode to about 49 kJ in the 64-lifter mode. The only exception is related to the 40-lifter mode, where the KE of the balls has increased compared to the 36-lifter mode, which may be due to the release of some balls trapped between the lifters from the mill wall (Figure 11). In general, there is an inverse relationship between the lifter count and the KE of the balls in the Hi-lo liner. In Figure 16e, it can be seen that by increasing the lifter count from 4 to 64, the PE of the balls has increased from about 588 kJ to about 656 kJ and there is a direct relationship between the lifter count and the PE of the balls in the Hi-lo liner. In this figure, like the corresponding figure in the Cuboid (Lo-lo) liner, two humps are observed in the 40-lifter and 48-lifter modes. In the 40-lifter mode (hump 1), as shown in Figure 11; the distance between the two lifters is twice the diameter of the balls, and in these distances, the balls are trapped two by two, and they are attached to the mill wall, so they rise to a higher height, and cause a sudden increase in the PE of the balls. The difference with the Lo-lo mode is that due to the change in the height of the lifters, some balls can release themselves from the wall of the mill and fall from a higher height. Also in the case of 48-lifters (hump 2), as shown in Figure 11, the distance between the lifters is equal to the diameter of a ball, and the balls get trapped in these distances and stick to the mill wall, which once more causes a sudden increase in the PE of the balls. One more time, due to the change in the height of the lifters, some of the balls can release themselves from these distances and fall from a higher height. Figure 16f also has a completely similar trend to Figure 16e. By simultaneously paying attention to Figures 11 and 16, that is, considering the role of the PE of the balls, creating suitable shoulder and toe points for them, as well as continuously creating cataracting motions for them, it can be concluded that the optimal lifter count for the studied mill is between 36 and 44 if Hi-lo liner is installed. Only in the 40-lifter mode, one should be careful not to trap the balls in the mill wall.

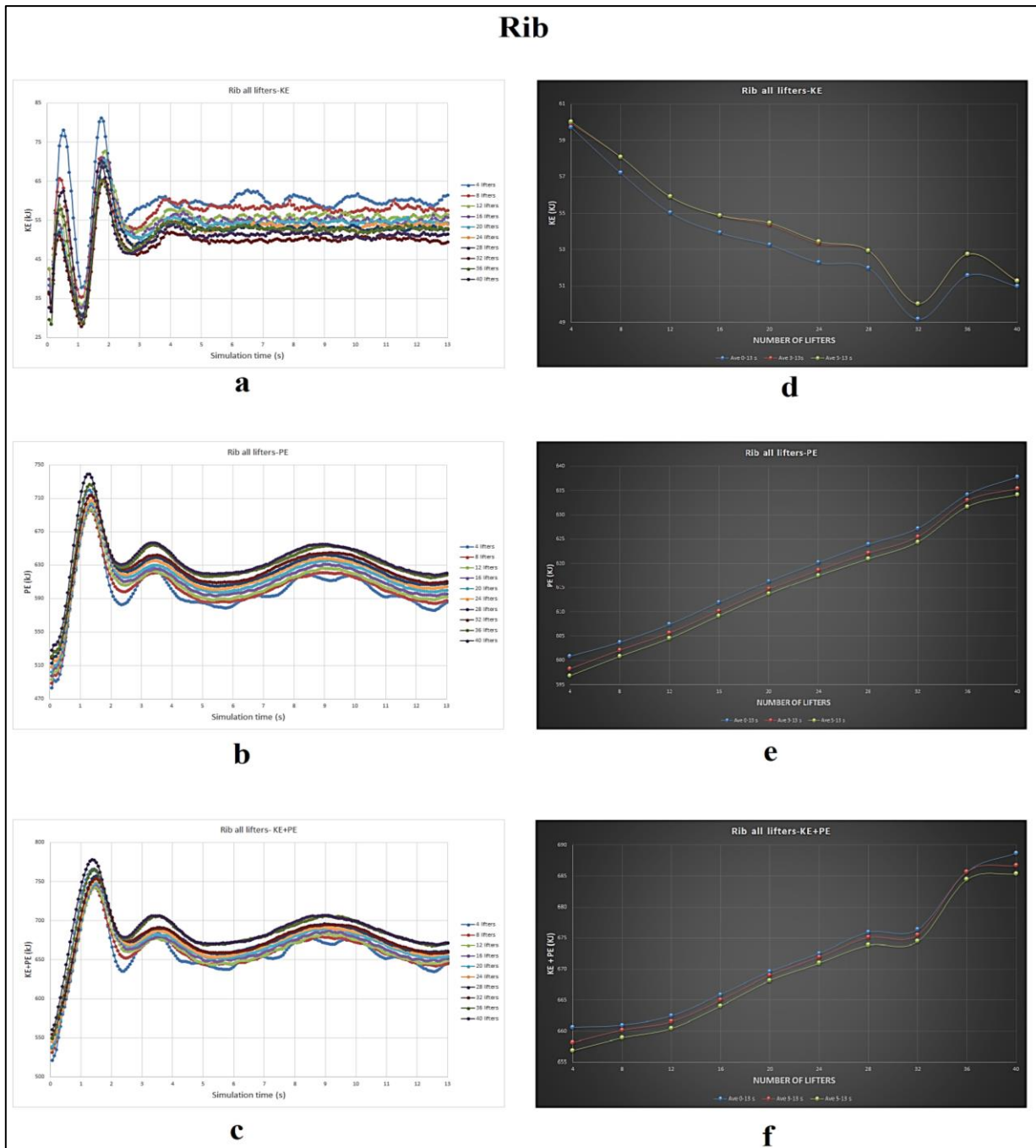


Figure 14. Values of a) *KE*, b) *PE*, c) *TE* d) the average of *KE* e) the average of *PE* and f) the average of *TE* of balls for the Rib liner from 4 to 40 lifters.

Figure 17 demonstrates the values of *KE*, *PE*, *TE* of balls, and their averages for Osborn liner from 4 to 120 lifters during simulation time from 0 to 13s. In Figure 17a), after starting the mill, the *KE* of the balls comes to its first maximum in about 0.5s for all modes from 4 to 120 lifters. Then it gets to its minimum in about 1.2s. Once more, it comes to its second maximum in about 1.6 s and reaches a relative steady state in about 2.3 s. In 4, 104, 108, 112, 116, and 120-lifter modes, there are a good many of fluctuations in the *KE* of the balls. In the 4-lifter mode, the reason for the fluctuations is the

small lifter count. However, in the 104-120 lifter modes, the reason for the fluctuations is the large lifter count and the decrease in their effect due to the reduction of their distance. In other words, in the 104 to 120 lifter modes, the mill operates similarly to a lifter-less mill with a smaller volume, which is not economically viable. In Figure 17b), after starting the mill, the *PE* of the balls gets to its maximum in about 1.2 s for all modes (from 4 to 120 lifters). Then it gets to its minimum in about 2.4s and comes to a steady state in about 3.5 s for most modes. In the 4, 100, 104, 108, 112, 116, and

120 lifter modes; there are many fluctuations in the *PE* of the balls, which is due to the small lifter count in the 4-lifter mode, and the large number of them in the 100–120 lifter modes, which makes the mill work like a lifter-less mill. Another noteworthy point is that in the 60- and 64-lifter modes, the *PE* of the balls has a sudden jump, and in the 64-lifter mode, a good many of fluctuations are also observed. In the 60-lifter mode, the reason is that the balls stick to the mill wall (Figure 12), but in the 64-lifter mode, the reason for the oscillation is that at some moments the cataract motions are interrupted, and there are only cascade motions. In other words, there are two modes of motion of the balls in the mill. It is worth mentioning that, among all the simulations performed in this research, this two-mode motion was observed only in the Osborn liner and for the 64-lifter mill. Figure 17c also has the same trend as Figure 17b. In Figure 17d, it can be seen that the *KE* of the balls has decreased from about 60 kJ to about 51 kJ in 4 to 48-lifter modes. Then it has increased from 48-lifter mode to 68-lifter mode and came to about 58.5 kJ. From 68 lifters to 100 lifters, a sharp decrease in the *KE* of the balls can be observed anew, so that their *KE* in the 100-lifter mode has reached 43 kJ. Once more, from the 100-lifter to 120-lifter mode, an increase in the *KE* of the balls is observed. In general, there is no specific trend for the *KE* of the balls, and in the Osborn liner, the *KE* of the balls cannot be used as a basis for analysis. In Figure 17e, it can be seen that with

the increase in the lifter count, the *PE* of the balls has increased and there is a direct relationship between them. But in the 60-lifter and 80-lifter modes, a sudden increase in the *PE* of the balls is observed and two humps can be seen in the graph. In the 60 lifter modes, as mentioned in Figure 12, the distance between the lifters is twice the diameter of the balls, and the balls are trapped in pairs in this distance and stick to the mill wall and as a result cause a sudden increase in the ball *PE*. In the 80-lifter mode, according to Figure 12, the distance between the lifters is equal to the diameter of a ball, and the balls are trapped individually in these distances, and once more a sudden increase in their *PE* is observed. Figure 17f also has a trend similar to Figure 17e. In general, for the optimal selection of the lifter count in the Osborn liner, the *PE* of the balls should be the basis of the analysis, and their *KE* will not help to make a decision. Also *PE* alone is not enough to choose the right lifter count, and creating cataracting motions in the mill as well as creating suitable shoulder and toe points for the balls should be considered simultaneously. In other words, a liner is suitable when its lifters provide both high *PE* for the balls and also create proper shoulder and toe points, and cataract motions. Considering the above, it can be said that the appropriate range of the lifter count for the Osborn liner in the mill studied in this research is between 52 and 88 lifters. Also, the optimal range is between 64 and 76 lifters.

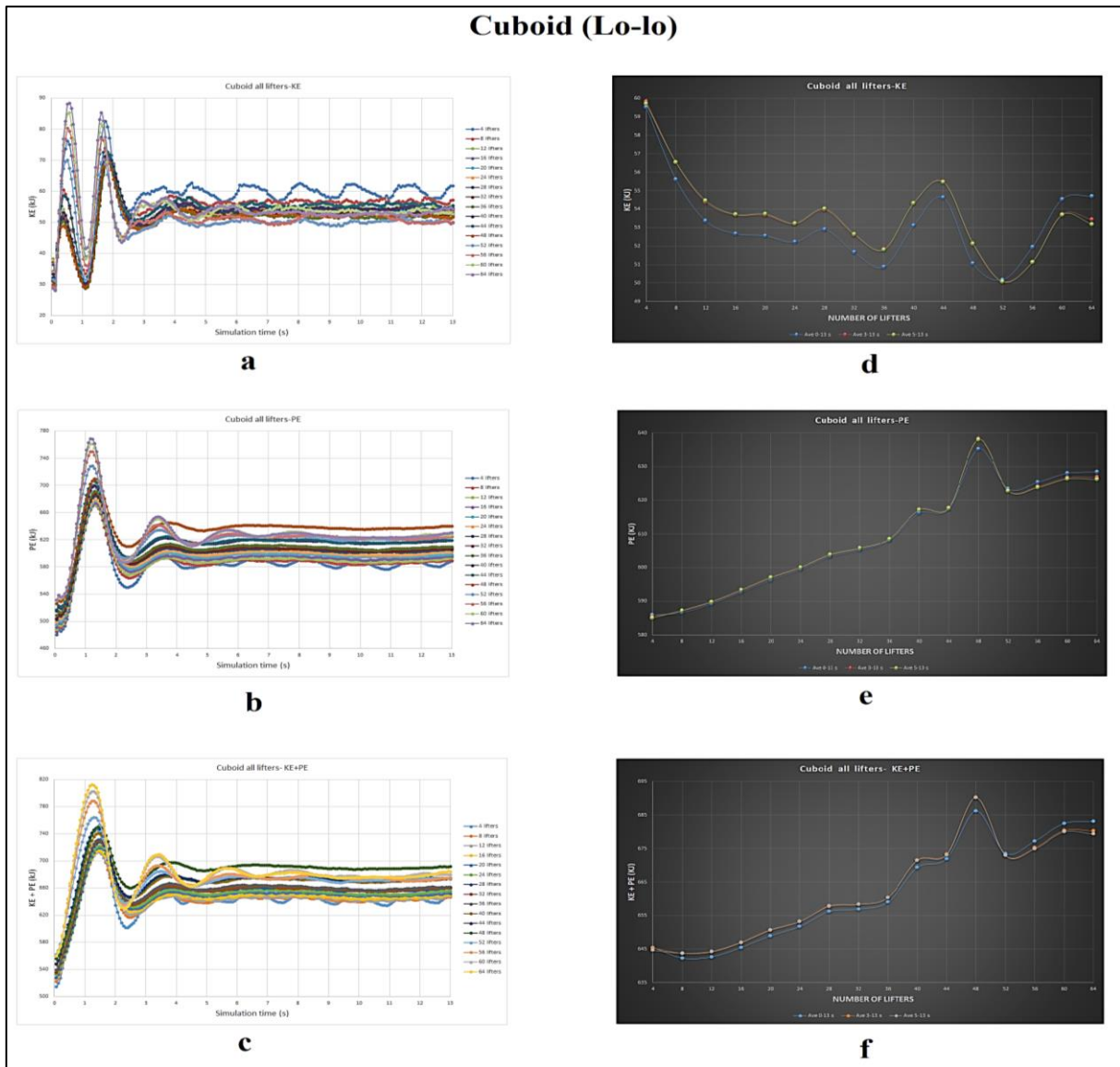


Figure 15. Values of a) *KE* b) *PE* c) *TE* d) the average of *KE* e) the average of *PE* and f) the average of *TE* of balls for Cuboid (Lo-lo) liner from 4 to 64 lifters.

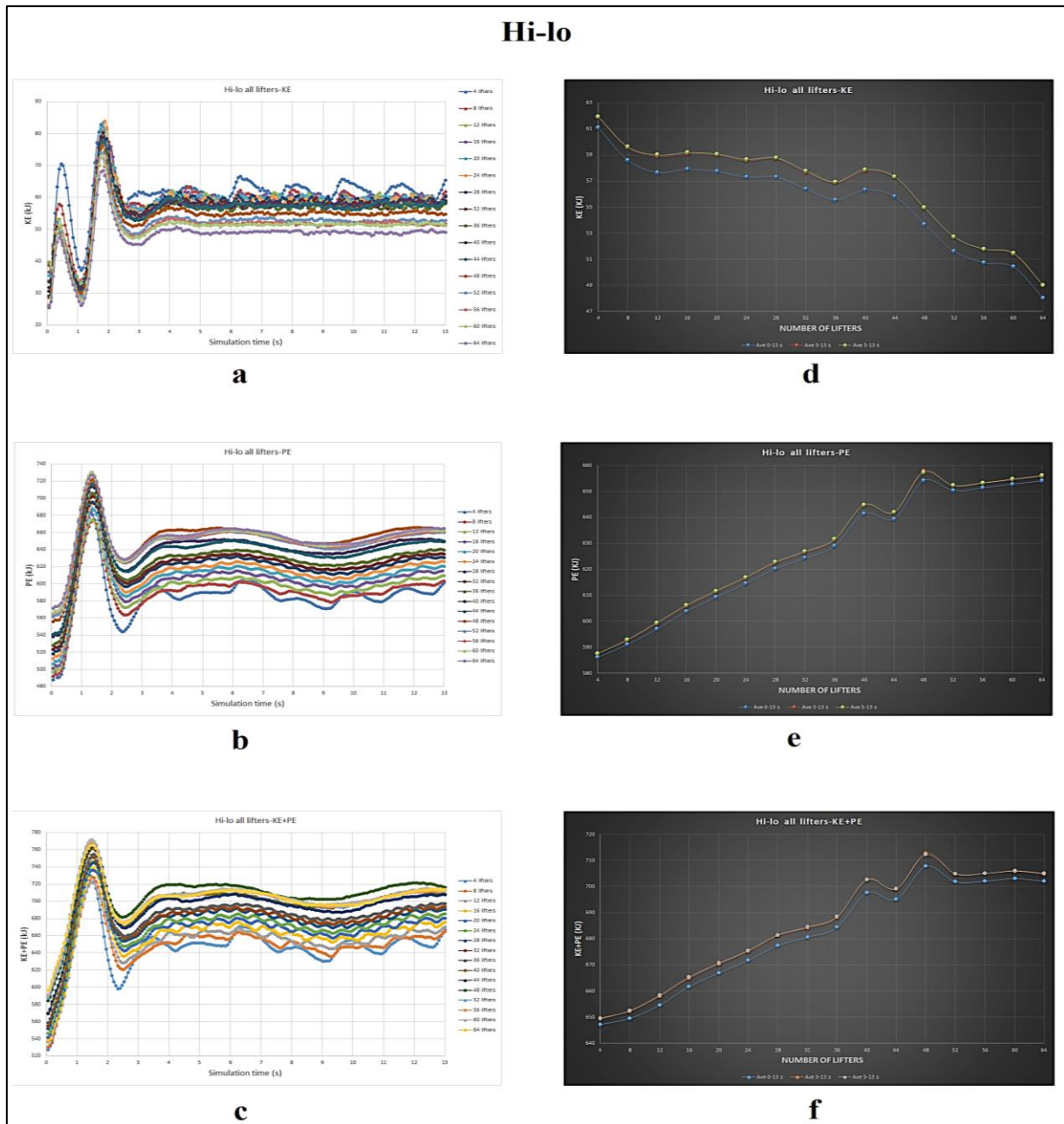


Figure 16. Values of a) KE b) PE c) T d) the average of KE e) the average of PE and f) the average of TE of balls for Hi-lo liner from 4 to 64 lifters.

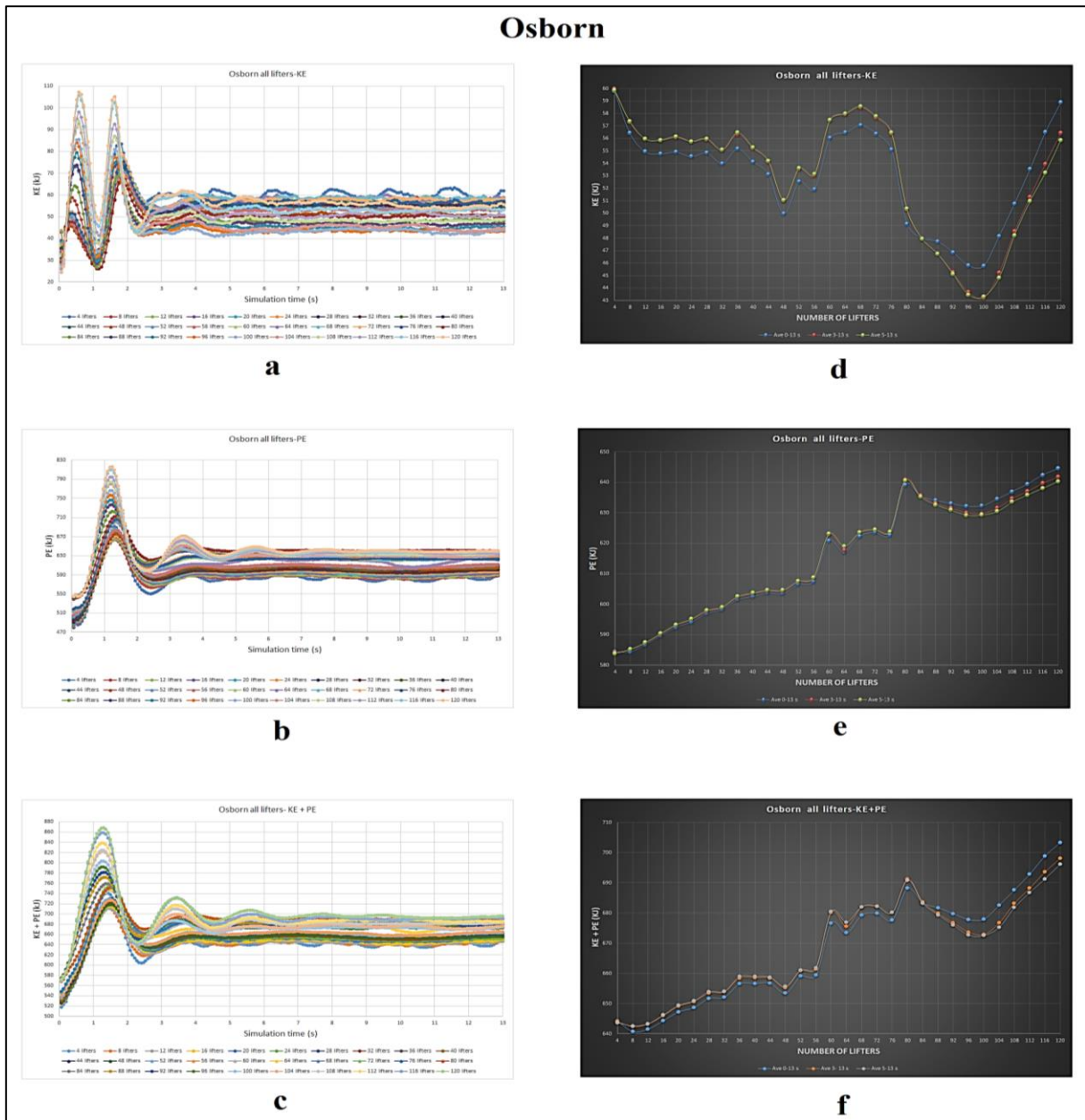


Figure 17. Values of a) *KE* b) *PE* c) *TE*, d) the average of *KE*, e) the average of *PE*, and f) the average of *TE* of balls for Osborn liner from 4 to 120 lifters.

Figure 18 compares the average of the value of *KE* (a), *PE* (b), and *TE* (c) of balls after the steady state (5-13s) in all five types of liners studied in this research work. In Figure 18a, in the Lorain liner, as the lifter count (*N*) increases from 4 to 24; the value of *KE* of the balls decreases linearly according to the following equation:

$$KE_{Lorain} (kJ) = -0.7394 N + 69.019$$

$$N = 4, 8, \dots, 24$$

$$R^2 = 0.9954$$

Also in the Rib liner, as the lifter count (*N*) increases from 4 to 40, the value of *KE* of the balls

decreases binomially according to the following equation:

$$KE_{Rib} (kJ) = 0.0067N^2 - 0.5258N + 61.816$$

$$N = 4, 8, \dots, 40$$

$$R^2 = 0.9279$$

In the cuboid (Lo-lo) liner, the relationship between the *KE* of the balls and the lifter count (*N*) is in the form of the following power equation:

$$KE_{Cuboid (Lo-lo)} (kJ) = 61.335N^{-0.04}$$

$$N = 4, 8, \dots, 64$$

$$R^2 = 0.6151$$

As can be seen, the coefficient of determination (R^2) in this case is very low, and it can be said that there is no special relationship between the lifter count (N) and the *KE* of the balls in the Cuboid liner.

In the Hi-lo liner, with the increase in the lifter count (N) from 4 to 64, the *KE* of the balls has decreased binomially according to the following formula:

$$KE_{Hi-lo} (kJ) = -0.0032N^2 + 0.0409N + 60.001$$

$$N = 4, 8, \dots, 64 \tag{8}$$

$$R^2 = 0.9378$$

Also in the Osborn liner, there is the following linear relationship between the *KE* of the balls and the lifter count (N):

$$KE_{Osborn} (kJ) = -0.0851x + 58.405$$

$$N = 4, 8, \dots, 120 \tag{9}$$

$$R^2 = 0.39$$

As can be seen, the coefficient of determination (R^2) between the *KE* of the balls and the lifter count in this case is too low, which indicates that there is no special relationship between them, and in the Osborn liner, the *KE* of the balls and the lifter count are almost independent from each other.

In Figure 18b in the Lorain liner, as the lifter count (N) increases from 4 to 24, the value of *PE* of the balls increases linearly according to the following equation:

$$PE_{Lorain} (kJ) = 4.2508N + 590.96$$

$$N = 4, 8, \dots, 24 \tag{10}$$

$$R^2 = 0.9998$$

Also in the Rib liner, as the lifter count (N) increases from 4 to 40, the value of *PE* of the balls increases linearly according to the following relationship:

$$PE_{Rib} (kJ) = 1.0455N + 592.39$$

$$N = 4, 8, \dots, 40 \tag{11}$$

$$R^2 = 0.9961$$

Also in the cuboid (Lo-lo) liner, with the increase in the lifter count (N) from 4 to 64, the *PE* of the balls has increased binomially according to the following equation:

$$PE_{Cuboid (Lo-lo)} (kJ) = -0.0054N^2 + 1.1728N + 577.13$$

$$N = 4, 8, \dots, 64 \tag{12}$$

$$R^2 = 0.9063$$

Also, in the Hi-lo liner, with the increase in the lifter count (N) from 4 to 64, the *PE* of the balls has increased binomially according to the following equation:

$$PE_{Hi-lo} (kJ) = -0.0117N^2 + 2.031N + 577.01$$

$$N = 4, 8, \dots, 64 \tag{13}$$

$$R^2 = 0.9795$$

Another noteworthy point in Figures 18a and b is that the *KE* and *PE* of the balls in the Hi-lo liner are higher than their corresponding values in the Lo-lo liner in almost all cases, which shows increasing the height of the lifters can increase the values of *KE*, and especially the *PE* of the balls.

Also, in Figure 18b in the Osborn liner, with the increase in the lifter count (N) from 4 to 120, the *PE* of the balls has increased binomially according to the following relationship:

$$PE_{Osborn} (kJ) = -0.0024N^2 + 0.8015N + 577.61$$

$$N = 4, 8, \dots, 120 \tag{14}$$

$$R^2 = 0.9483$$

In general, the *PE* of the balls in all five types of liners investigated increases with the increase in the lifter count, and there is a direct relationship between them. The high coefficient of determination (R^2) between the *PE* of the balls and the lifter count in all five types of liners shows that the *PE* of the balls is a suitable criterion for choosing the optimal lifter count, and should be used as a basis for decision-making.

In Figure 18c, in the Lorain liner, with the increase in the lifter count from 4 to 24 (N), the *TE* of the balls has increased linearly according to the following formula:

$$TE_{Lorain} (kJ) = 3.5114N + 659.98$$

$$N = 4, 8, \dots, 24 \tag{15}$$

$$R^2 = 0.9996$$

Also in the Rib liner, with the increase in the lifter count (N) from 4 to 40, the *TE* of the balls has increased binomially according to the equation below:

$$TE_{Rib} (kJ) = 0.0083N^2 + 0.4503N + 654.76 \tag{16}$$

$$N = 4, 8, \dots, 40$$

$$R^2 = 0.9774$$

Also in the cuboid (Lo-lo) liner, with the increase in the lifter count (N) from 4 to 64, the TE of the balls has increased binomially according to the following equation:

$$TE_{\text{Cuboid (Lo-lo)}} \text{ (kJ)} = -0.0024N^2 + 0.8917N + 635.9$$

$$N = 4, 8, \dots, 64 \tag{17}$$

$$R^2 = 0.8707$$

Also in the Hi-lo liner, with the increase in the lifter count from 4 to 64 (N), the TE of the balls has increased binomially according to the following formula:

$$TE_{\text{Hi-lo}} \text{ (kJ)} = -0.0149N^2 + 2.0718N + 637.01 \tag{18}$$

$$N = 4, 8, \dots, 64$$

$$R^2 = 0.9669$$

Once more, it can be seen that the TE of the Hi-lo liner is higher than the Lo-lo liner in all modes, which indicates the positive effect of increasing the height of the lifters on the TE of the balls.

In Figure 18c, in the Osborn liner, with the increase in the lifter count from 4 to 120 (N), the TE of the balls has increased binomially according to the following formula:

$$TE_{\text{Osborn}} \text{ (kJ)} = -0.0023N^2 + 0.6975N + 636.42$$

$$N = 4, 8, \dots, 120 \tag{19}$$

$$R^2 = 0.853$$

As can be seen, in all cases, the coefficients of determinations (R^2) between the TE of the balls and the lifter count are lower than the corresponding values for the PE, which indicates that the PE of the balls is a more appropriate criterion for choosing the optimal range of the lifter count.

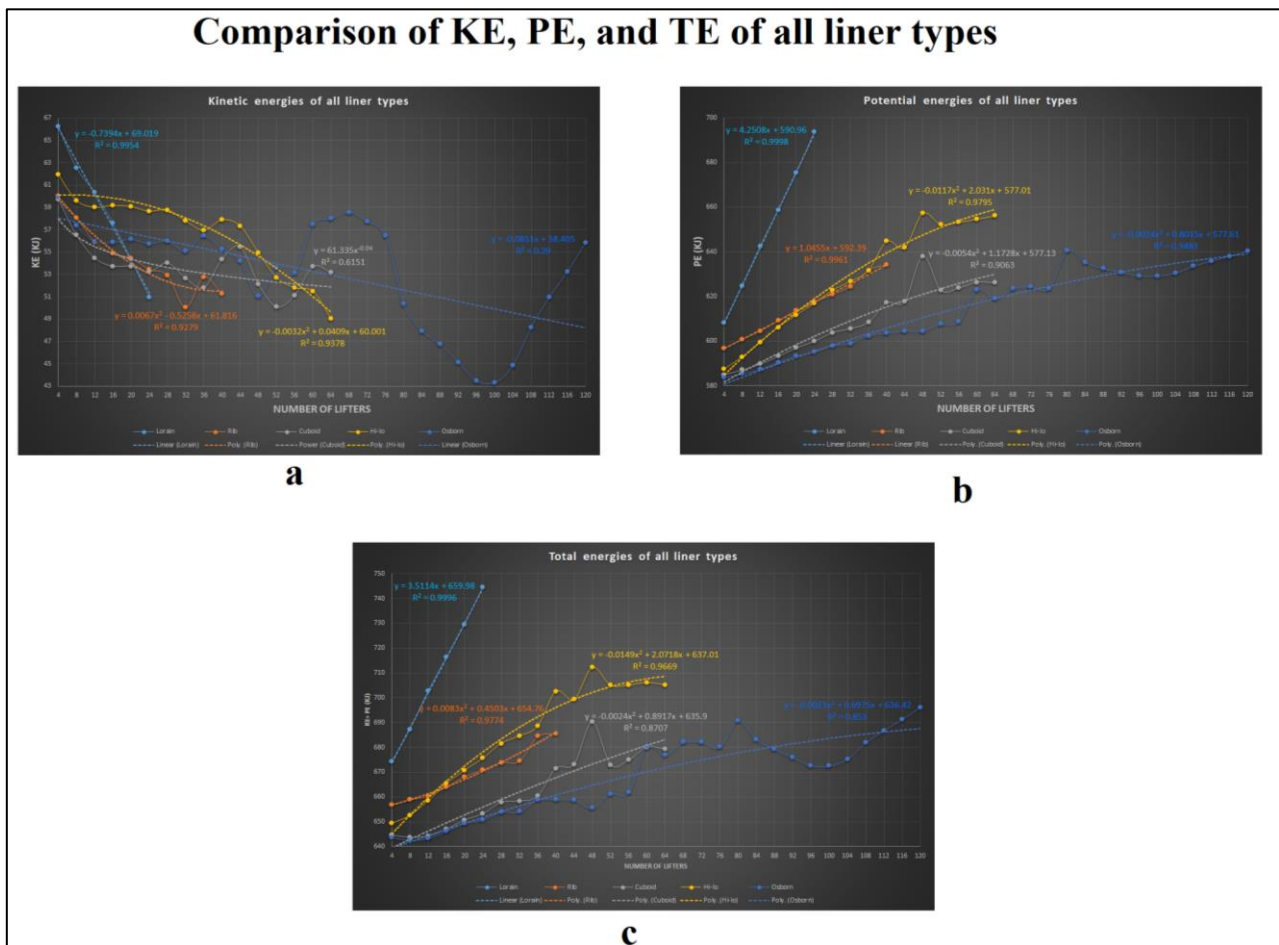


Figure 18. Comparison of the average of the value of KE (a) PE (b) and TE (c) of balls in all five types of liners.

4. Comparison between Experimental Results and DEM Predictions

Experimental validation of *DEM* simulations is an important step to guarantee that the system is well described and that the predictions are close to the real operating conditions. The power draw is the principal parameter used to validate *DEM* simulations (Pérez-Alonso and Delgadillo, 2012).

In this research work, in order to validate the simulation results, the industrial mill of Meskavan Company (Abbas Abad, Shahrood, Iran) with dimensions of 3.28×5.10 was simulated. Figure 19 compares the two-dimensional profile and three-dimensional geometry of the lifter of Meskavan Company ball mill with the five lifters investigated in this research. Figure 20 shows the exact geometrical characteristics of the ball mill lifters of Meskavan Company. Figure 21 demonstrates the 3D geometries of the Meskavan

Company ball mill with Pseudo- Lorain liner with 24 lifters. As can be seen from Figures 19–21, the length of the Meskavan lifter (5.10 m) is shorter than that of all the lifters studied in this research work (5.70 m). Its width (0.16 m) is almost equal to the width of cuboid and Hi (0.14 m) lifters. Its height (0.09 m) is higher than the height of the cuboid (0.07 m) and Rib (0.06 m) lifters, and is almost equal to the height of the Osborn lifter (0.08 m). But it has a much lower height than Hi (0.14 m) and Lorain (0.15 m) lifters. The geometric shape of its profile is almost the same as Lorain lifter. With the difference that this lifter is not symmetrical, and its left side has a greater slope (60°) than its right side (45°). Therefore, we named it pseudo-Lorain. Tables 7–10 tabulated the detailed operating and geometric conditions, material properties, and calculations for the Meskavan Company ball mill.

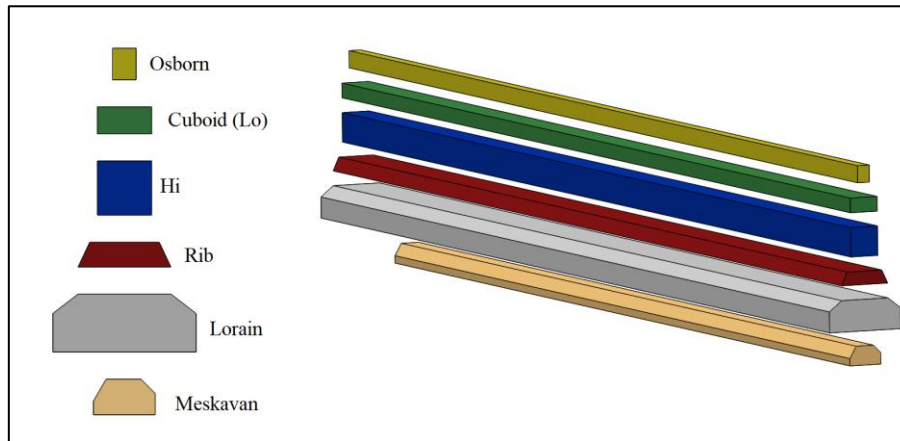


Figure 19. Comparison of the 2D profile and 3D geometry of the lifter of Meskavan Company ball mill with other lifters studied in this research work.

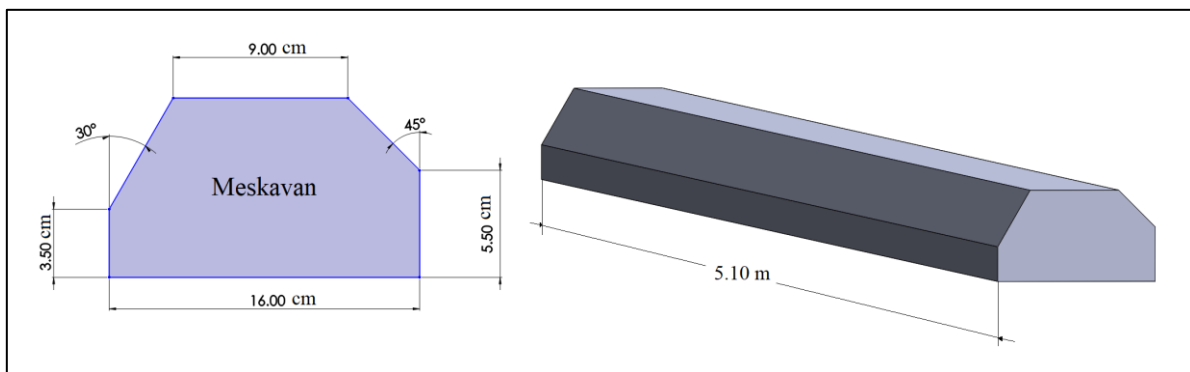


Figure 20. Precise geometric dimensions of ball mill lifters of Meskavan Company.

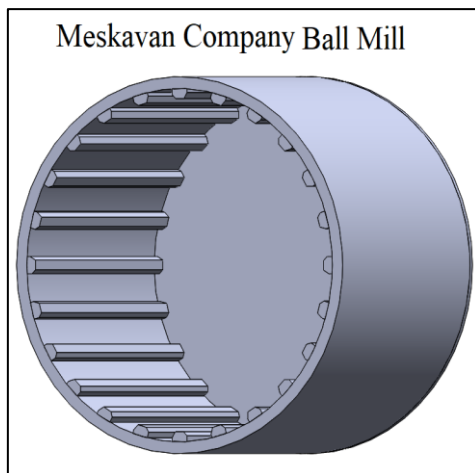


Figure 21. 3D geometry of the Meskavan Company ball mill with Pseudo Lorain liner with 24 lifters.

Table 7. Dimensions and velocities of the Meskavan Company ball mill.

Meskavan Company ball mill	Value
Mill inside length (m)	5.10
Mill inside diameter (m)	3.28
Mill volume without lifters (m ³)	43.09310= 43.09
Critical speed (CS) (rpm)	23.57
Mill rotation speed (71.27% of CS) (rpm)	16.80
Mill rotation direction	Clockwise

Table 8. DEM ball Size distribution and Specification inside Meskavan Company ball mill.

Ball size class (mm)	Mass fraction (%)
60	53
50	29
40	13
30	5

Table 9. Calculations and specifications of DEM balls of Meskavan mill.

Volume of a single 60-mm ball (m ³)	$1.13097 \times 10^{-4} = 1.13 \times 10^{-4}$
Volume of a single 50-mm ball (m ³)	$6.54498 \times 10^{-5} = 6.54 \times 10^{-5}$
Volume of a single 40-mm ball (m ³)	$3.35103 \times 10^{-5} = 3.35 \times 10^{-5}$
Volume of a single 30-mm ball (m ³)	$1.41372 \times 10^{-5} = 1.41 \times 10^{-5}$
Filling of mill ball charge (%)	34.5536% = 34.55%
Volume of all balls (m ³)	$34.5536\% / 2 \times 43.09310 = 7.44512 = 7.44$
Number of 60-mm balls in simulation	$(7.44512 \times 0.53) / 1.13097 \times 10^{-4} = 34890$
Number of 50-mm balls in simulation	$(7.44512 \times 0.29) / 6.54498 \times 10^{-5} = 32988$
Number of 40-mm balls in simulation	$(7.44512 \times 0.13) / 3.35103 \times 10^{-5} = 28883$
Number of 30-mm balls in simulation	$(7.44512 \times 0.05) / 1.41372 \times 10^{-5} = 26332$
Total number of balls in simulation	123092
Ball density (kg/m ³)	8050
Total mass of balls (kg)	$8050 \times 7.44512 = 59933.19549 = 59933.20$

Table 10. Parameters of DEM simulation of Meskavan mill.

DEM model details	Value
DEM spring constant (kg/m)	10 ⁶
Ball sliding friction coefficient	0.5
Ball rolling friction coefficient	0.0015
Poissons ratio	0.285
Young's modulus (N/m ²)	1×10 ⁹
Ball restitution coefficient	0.817
Time step (s)	0.0001=10 ⁻⁴
Period of 71.27% CS	60/16.8 = 3.5714
Particle interaction distance (m)	5% × 15 mm = 7.5 × 10 ⁻⁴

Figure 22 demonstrates the real profile of the rubber lifters of the Meskavan ball mill. The length of the lifters is about one meter, and by placing five of them next to each other, the entire length of the mill is covered (Figure 23). Figure 23 shows how to install liners and lifters designed by our team (authors of the article) inside the Meskavan ball mill. After the installation of these pseudo-Lorain lifters, the throughput of the mill increased by about 20%, which was due to the decrease in the retention time of the particles due to the appropriate design of the lifters' profile and their appropriate number (24 pieces). Figure 24 demonstrates the data of the control room related to the grinding circuit of the ball mill of Meskavan Company. Figure 24a corresponds to time 0s. The

data related to the mill motor such as amperage (A), power draw (kW), motor revolution (rpm), and torque (N.m) were accessible at one second intervals from the control room of the plant. Figure 24b shows the data related to the ball mill motor including amperage, power draw, motor revolution, and torque (N.m) at times 0–13s after starting the mill. These values can be seen in Table 11. As it is clear, there is a direct relationship between amperage, power draw, motor revolution and torque. After starting the mill, all these values have come to their maximum in about 1s. Then they got to their minimum in around 2s and after the mill reached a steady state in about 5s, they have remained almost constant until 13s.



Figure 22. Real profile of the rubber lifters of the Meskavan ball mill.



Figure 23. Installation of designed liners and lifters of the Meskavan ball mill.

Table 11. Control room data of Meskavan ball mill.

Time (s)	amperage (A)	Power (kW)	Motor revolution (rpm)	Torque (N.m)
0	1227.3	643	1470	4173
1	1345.6	715	1493	4573
2	1205.1	627	1440	4155
3	1215.2	636	1439	4220
4	1298.1	670	1470	4352
5	1300.4	675	1471	4384
6	1315.7	678	1470	4406
7	1285.5	679	1494	4342
8	1294.9	688	1495	4397
9	1294.1	681	1493	4355
10	1304.7	681	1470	4422
11	1292.8	683	1494	4364
12	1299.1	683	1495	4362
13	1314.1	683	1494	4369

Figure 25 displays DEM simulation of the Meskavan ball mill with the 24 pseudo-Lorain lifters. As it can be seen, cascading and cataracting motions, as well as suitable shoulder and toe points

for the balls have been created, which indicates that the lifter count (24 pieces) as well as their width and height are suitable and shows their good design.

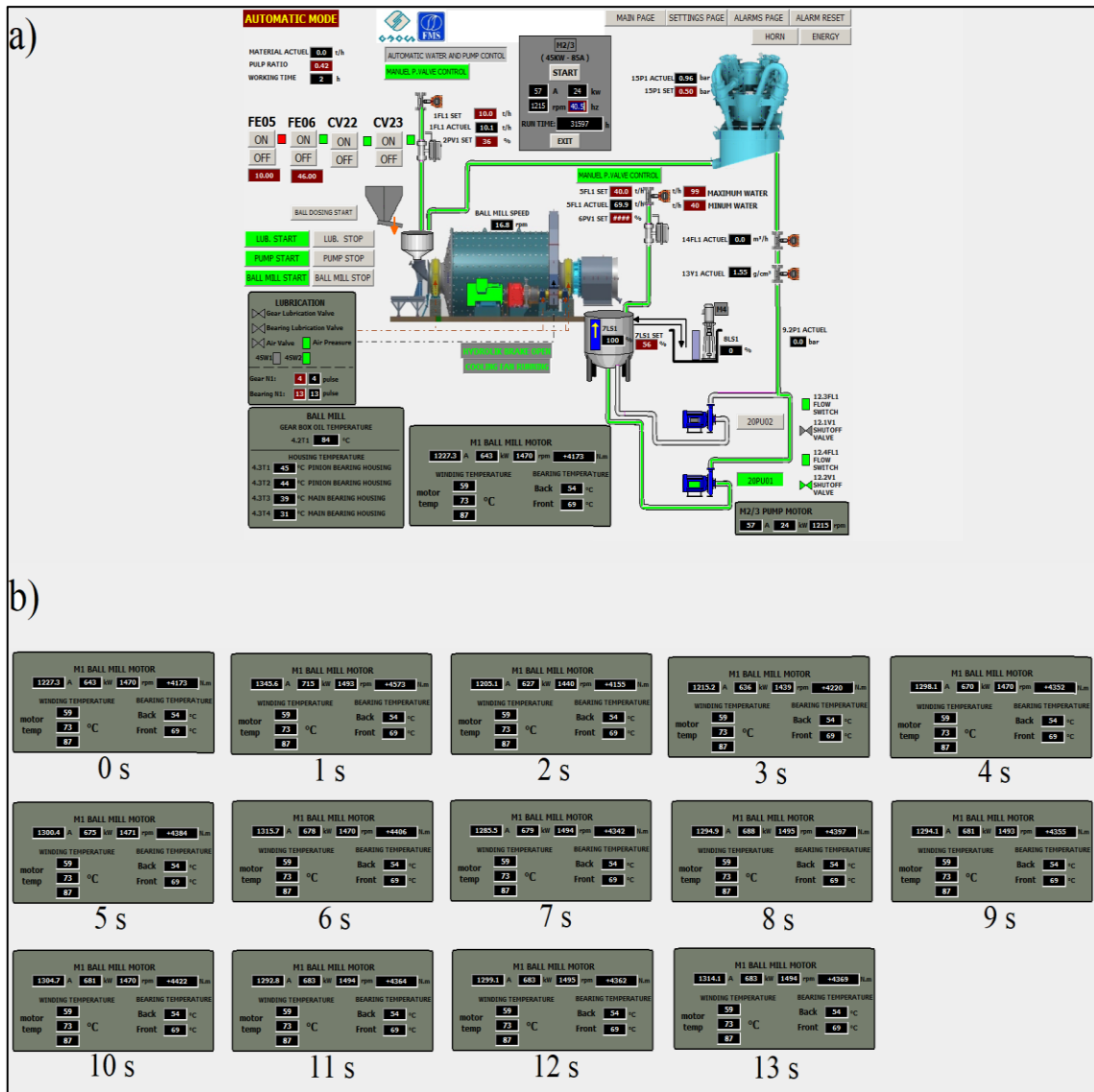


Figure 24. a) Data of the control room related to the grinding circuit of the ball mill of Meskavan Company. b) Data related to the ball mill motor of Meskavan Company including amperage (A), power draw (kW), motor revolution (rpm), and torque (N.m) at times 0–13s after starting the mill.

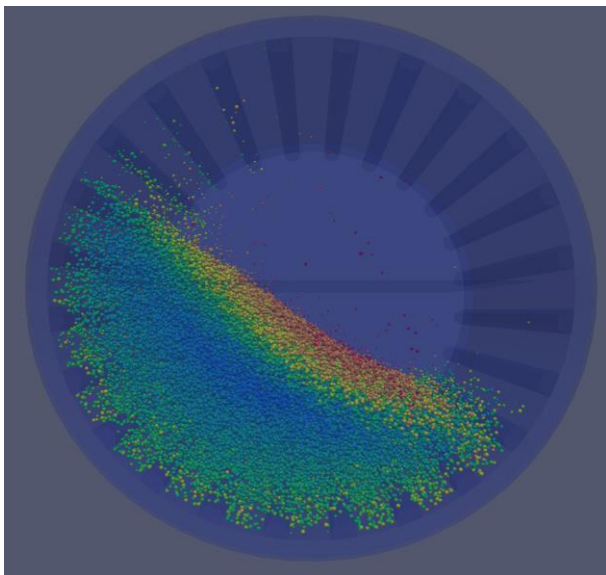


Figure 25. DEM simulation of the Meskavan ball.

Figure 26 compares the values of KE , PE , and TE of the balls in the ball mill of Meskavan Company obtained by DEM simulation. As can be seen, in the Meskavan ball mill, as in other cases (Lorain, Rib, ...) examined in this research work, the value of PE of the balls is much higher than their KE . As a result, for this mill PE should be the basis of decision making as well. Also Equations 20 and 21 show how to calculate KE and PE for a single ball i at Meskavan mill. Equations 22 and 23 also indicate how to calculate these energies for all balls (123092) of the Meskavan Company ball mill.

$$KE_i = \frac{1}{2} m_i V_i^2 \quad (20)$$

$$i = 1, 2, \dots, 123092$$

$$PE_i = m_i g h_i \tag{21}$$

$i = 1, 2, \dots, 123092$

$$KE = \sum_{i=1}^{123092} KE_i \tag{22}$$

$$PE = \sum_{i=1}^{123092} PE_i \tag{23}$$

Figure 27 compares the values of actual power draw of Meskavan mill (kW) with the values of *KE*, *PE*, and *TE* of the balls in *DEM* simulations. Power

draw values could only be measured in one-second time intervals for the Meskavan mill, and therefore, only 14 data were available for them. However, in *DEM* simulations, data are available at all moments, and there are 200 data in a 13-second period. It is noteworthy that the values of the power draw of the Meskavan mill (in wet state (ball + pulp)) are very close to the values of the *PE* of the balls (in dry state (ball only)), especially after reaching a steady state (5 to 13s), which once again proves that in *DEM* simulations, the *PE* of particles should be the basis for estimating the power draw of mills.

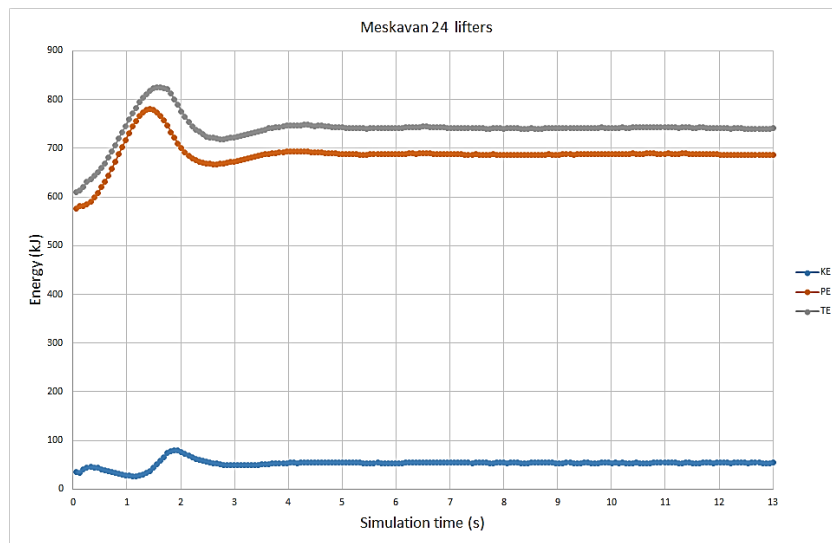


Figure 26. Comparison of *KE*, *PE*, and *TE* values of the balls in the ball mill of Meskavan Company using *DEM*.

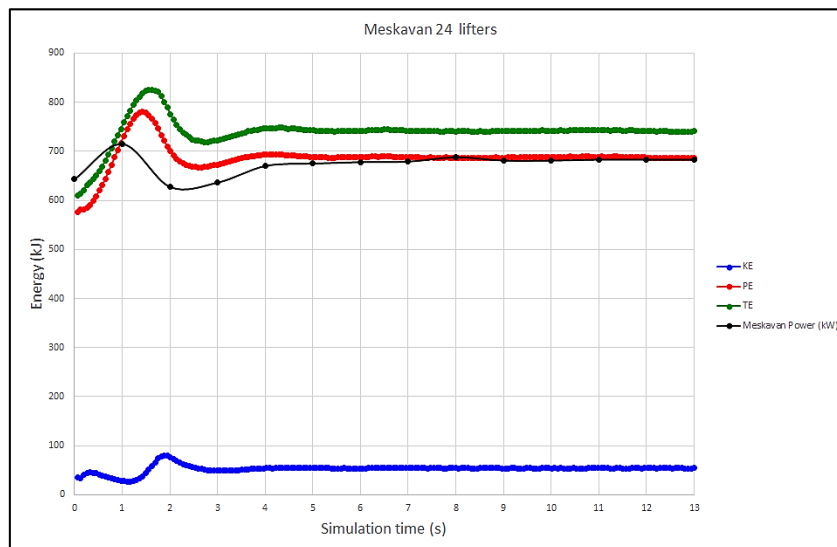


Figure 27. Comparison of the actual power draw of the Meskavan ball mill (kW) with the values of *KE*, *PE*, and *TE* of the balls in *DEM* simulation.

5. Conclusions

In this research work, for the first time, the *KE*, *PE*, and *TE* of all the balls inside a good many of

industrial-scale ball mills were calculated in the entire duration of the *DEM* simulations from 0–13s. In Part 1 of this research work, five types of liners, i.e. Lorain, Osborn, Rib, cuboid, and Hi-lo,

were examined. Also their corresponding graphs for all five types of liners and all lifter numbers from four upwards were drawn and compared in details. On the other hand, using data related to these energies, for each type of liner, the optimal lifter count was obtained. Also in order to validate the simulation results, the power draw of Meskavan ball mill was compared with the *KE*, *PE*, and *TE* of all the balls obtained from *DEM* simulation, which showed a good agreement.

Also the following practical and valuable results were obtained from this research work:

- Considering the proper performance of Lorain and Rib liners in all modes, it can be concluded that the trapezoidal profile is suitable for industrial ball mill liners.
- A sudden increase in the *PE* of the balls indicates that they are trapped at the distances between the lifters and are stuck to the mill wall and practically do not participate in grinding.
- When the *KE* of the balls has less fluctuations, the number of mill lifters is suitable. On the contrary, when the fluctuations of *KE* are high, it indicates that the lifter count is not enough and the motion of the balls in the mill is not uniform and stable. Also from the fluctuations of the *PE* of the balls, it is possible to find out whether the lifter count is sufficient or not.
- By comparing the values of *KE* and *PE*, it can be concluded that the value of *PE* is much higher than that of *KE*. This shows that *PE* is more important than *KE* and lifters, which can raise the balls to a higher height are more suitable.
- If the height of the lifter is less than a certain limit, it will take longer than normal for the mill to get to a steady state. In general, mill performance can be improved by increasing lifter height.
- As the lifter count increases, because they raise the balls to a higher height, *PE* increases, and there is a direct relationship between the lifter count and *PE*.
- When observing a sudden jump (humps) in the *PE* diagram of the balls, their adhesion to the wall of the mill should be checked. and this issue should be avoided.
- *PE* to some extent can help to choose the optimal lifter count. As such choosing the optimal lifter count should be done considering the creation of cataracting motions, the creation of appropriate shoulder and toe points, and the *PE* of the balls simultaneously.
- 16 to 20 lifters were recommended for the Lorain liner, 64 to 76 lifters for the Osborn liner, 24 to

32 lifters for the Rib liner, 44 lifters for the Cuboid (Lo-lo) liner, and 36 to 44 lifters for the Hi-lo liner.

- *KE* and *PE* values in the Hi-lo liner were higher than their corresponding values in the Lo-lo liner in almost all cases, which indicates that increasing the height of the lifters can increase the values of *KE* and especially *PE*.
- *PE* in all five types of investigated liners increased with the increase in the lifter count, and there was a direct relationship between them. The high coefficient of determination (R^2) between *PE* and the lifter count in all five types of liners showed that *PE* is a suitable criterion for choosing the optimal lifter count, and should be used as a basis for decision-making.
- In the Meskavan ball mill, as in other cases examined in this research work, the value of *PE* was much higher than *KE*. As a result, for this mill, *PE* should be the basis of decision-making as well.
- After the installation of the pseudo-Lorain lifters designed by us, the throughput of the Meskavan ball mill increased by about 20%, which was due to the decrease in the retention time of the particles due to the appropriate design of the lifters' profile and their appropriate number (24 pieces).
- With comparing the values of actual power draw of the Meskavan ball mill (kW) (in wet state (ball + pulp)) with the values of *KE*, *PE*, and *TE* of the balls in *DEM* simulations (in dry state (ball only)), it can be concluded that the values of the power draw of the Meskavan mill are very close to the values of the *PE* of the balls, especially after reaching a steady state (5–13s), which once again proves that in *DEM* simulations, the *PE* of particles should be the basis for estimating the power draw of mills.

Acknowledgements

The authors would like to thank Shahrood University of Technology and the Meskavan Company (Abbas Abad, Shahrood) for their support.

References

- [1]. Makokha, A.B., Moys, M.H., Bwalya, M.M., & Kimera, K. (2007). A new approach to optimising the life and performance of worn liners in ball mills: Experimental study and DEM simulation. *International Journal of Mineral Processing*, 84, 221–227.
- [2]. Lee, H., Kim, K., & Lee, H. (2019). Analysis of grinding kinetics in a laboratory ball mill using

- population-balance-model and discrete-element-method. *Advanced Powder Technology*, 30, 2517–2526.
- [3]. Rosales-Marín, G., Andrade, J., Alvarado, G., Delgadillo, G.A., & Tuzcu, E.T. (2019). Study of lifter wear and breakage rates for different lifter geometries in tumbling mill: Experimental and simulation analysis using population balance model. *Minerals Engineering*, 141, 105857.
- [4]. Yahyaei, M., Powel, M.S., Toor, P., Tuxford, A., & Limpus, A. (2015). Relining efficiency and liner design for improved plant performance. *Minerals Engineering*, 83, 64–77.
- [5]. Yin, Z., Peng, Y., Zhu, Z., Yu, Z., & Li, T. (2017). Impact load behavior between different charge and lifter in a laboratory-scale mill. *Materials*, 10(8), 882.
- [6]. Mishra, B.K., & Rajamani, R.K. (1992). The discrete element method for the simulation of ball mills. *Applied Mathematical Modelling*, 16(11), 598–604.
- [7]. Mishra, B.K., & Rajamani, R.K. (1993). Numerical simulation of charge motion in ball mills—Lifter bar effect. *Mining, Metallurgy & Exploration*, 10, 86–90.
- [8]. Mishra, B.K., & Rajamani, R.K. (1994a). Simulation of charge motion in ball mills. Part 1: experimental verifications. *International Journal of Mineral Processing* 1994a, 40, 171–186.
- [9]. Mishra, B.K., & Rajamani, R.K. (1994b). Simulation of charge motion in ball mills. Part 2: numerical simulations. *International Journal of Mineral Processing*, 40, 187–197.
- [10]. Agrawala, S., Rajamani, R.K., Songfack, P., & Mishra, B.K. (1997). Mechanics of media motion in tumbling mills with 3d discrete element method. *Minerals Engineering*, 10(2), 215–227.
- [11]. Radziszewski, P. (1999). Comparing three DEM charge motion models. *Minerals Engineering*, 12(12), 1501–1520.
- [12]. Cleary, P.W. (1998). Predicting charge motion, power draw, segregation and wear in ball mills using discrete element methods. *Minerals Engineering*, 11, 1061–1080.
- [13]. Cleary, P.W. (2001a). Charge behaviour and power consumption in ball mills: sensitivity to mill operating conditions, liner geometry and charge composition. *International Journal of Mineral Processing*, 63, 79–114.
- [14]. Cleary, P.W. (2001b). Modelling comminution devices using DEM. *International Journal for numerical and analytical methods in geomechanics*, 25, 83–105.
- [15]. Monama, G.M., & Moys, M.H. (2002). DEM modelling of the dynamics of mill startup. *Minerals Engineering*, 15, 487–492.
- [16]. Hlungwani, O., Rikhotso, J., Dong, H., & Moys, M.H. (2003). Further validation of DEM modeling of milling: effects of liner profile and mill speed. *Minerals Engineering*, 16, 993–998.
- [17]. Djordjevic, N. (2003a). Discrete element modelling of the influence of lifters on power draw of tumbling mills. *Minerals Engineering*, 16, 331–336.
- [18]. Djordjevic, N. (2003b). Discrete element modelling of power draw of tumbling mills. *Mineral Processing and Extractive Metallurgy*, 112(2), 109–114.
- [19]. Djordjevic, N. (2003c). Discrete element modelling of lifter stresses in tumbling mill. *Mineral Processing and Extractive Metallurgy*, 112(2), 115–119.
- [20]. Mishra, B.K. (2003a). A review of computer simulation of tumbling mills by the discrete element method: Part I— contact mechanics. *International Journal of Mineral Processing*, 71, 73– 93.
- [21]. Mishra, B.K. (2003b). A review of computer simulation of tumbling mills by the discrete element method: Part II—Practical applications. *International Journal of Mineral Processing*, 71, 95–112.
- [22]. Powell, M.S., & McBride, A.T. (2004). A three-dimensional analysis of media motion and grinding regions in mills. *Minerals Engineering*, 17, 1099–1109.
- [23]. Makokha, A.B., & Moys, M.H. (2006). Towards optimising ball-milling capacity: Effect of lifter design. *Minerals Engineering*, 19, 1439–1445.
- [24]. Rezaeizadeh, M., Fooladi, M., Powell, M.S., & Mansouri, S.H. (2010). Experimental observations of lifter parameters and mill operation on power draw and liner impact loading. *Minerals Engineering*, 23, 1182–1191.
- [25]. Pérez-Alonso, C., & Delgadillo, J.A. (2012). Experimental validation of 2D DEM code by digital image analysis in tumbling mills. *Minerals Engineering*, 25, 20–27.
- [26]. Rajamani, R.K., Rashidi, S., & Dhawan, N. (2014). Advances in discrete element method application to grinding mills. *Mineral Processing and Extractive Metallurgy*, 100, 117–128.
- [27]. Bbosa, L.S., Govender, I., & Mainza, A. (2016). Development of a novel methodology to determine mill power draw. *International Journal of Mineral Processing*, 149, 94–103.
- [28]. Boemer, D., & Ponthot, J.P. (2017). DEM modeling of ball mills with experimental validation: influence of contact parameters on charge motion and power draw. *Computational Particle Mechanics*, 4, 53–67.
- [29]. Peng, Y., Li, T., Zhu, Z., Zou, S., & Yin, Z. (2017). Discrete element method simulations of load behavior with mono-sized iron ore particles in a ball mill.

Advances in Mechanical Engineering, 9(5), 1687814017705597.

[30]. Bian, X., Wang, G., Wang, H., Wang, S., & Lv, W. (2017). Effect of lifters and mill speed on particle behaviour, torque, and power consumption of a tumbling ball mill: Experimental study and DEM simulation. *Minerals Engineering*, 105, 22–35.

[31]. Sun, Y., Liang, M., Jin, X., Ji, P., & Shan, J. (2017). Experimental and modeling study of the regular polygon angle-spiral liner in ball mills. *Chinese Journal of Mechanical Engineering*, 30(2), 363–372.

[32]. Pedrayes, F., Normiella, J.G., Melero, M.G., Menéndez-Aguado, J.M., Juan, J.J., & del Coz-Díaz, J. (2018). Frequency domain characterization of torque in tumbling ball mills using DEM modelling: Application to filling level monitoring. *Powder Technology*, 323, 433–444.

[33]. Li, Z., Wang, Y., Li, K., Lin, W., & Tong, X. (2018). Study on the performance of ball mill with liner structure based on DEM. *Journal of Engineering & Technological Sciences*, 50(2).

[34]. Panjipour, R., & Barani, K. The effect of ball size distribution on power draw, charge motion and breakage mechanism of tumbling ball mill by discrete element method (DEM) simulation. *Physicochemical Problems of Mineral Processing*, 54(2), 258–269.

[35]. Li, G., Roufail, R., Klein, B., Zhou, L., Kumar, A., Sun, C., Kou, J., & Yu, L. (2019). Investigations on the charge motion and breakage effect of the magnetic liner mill using DEM. *Mining, Metallurgy & Exploration*, 36, 1053–1065.

[36]. Chimwani, N., & Bwalya, M.M. (2020). Using DEM to investigate how shell liner can induce ball segregation in a ball mill. *Minerals Engineering*, 151, 106311.

[37]. Góralczyk, M., Krot, P., Zimroz, R., & Ogonowski, S. (2020). Increasing energy efficiency and productivity of the comminution process in tumbling mills by indirect measurements of internal dynamics—an overview. *Energies*, 13, 6735.

[38]. Shahbazi, B., Jafari, M., Parian, M., Rosenkranz, J., & Chehreh Chelgani, S. (2020). Study on the impacts of media shapes on the performance of tumbling mills – A review. *Minerals Engineering*, 157, 106490.

[39]. AmanNejad, M., & Barani, K. (2021). Effects of Ball Size Distribution and Mill Speed and Their Interactions on Ball Milling Using DEM. *Mineral Processing and Extractive Metallurgy Review*, 42(6), 374–379.

[40]. Kolahi, S., Jahani Chegeni, M., & Seifpanahi-Shabani, K. (2021). Investigation of the effect of industrial ball mill liner type on their comminution mechanism using DEM. *International Journal of Mining and Geo-Engineering*, 55(2), 97–107.

[41]. Jahani Chegeni, M., & Kolahi, S. (2021). Determining an Appropriate range for the Number of Cuboid Lifters in Ball Mills using DEM. *Journal of Mining and Environment*, 12(3), 845–862.

[42]. Safa, A., & Sahraoui, A. (2023). Exploring the effects of a new lifter design and ball mill speed on grinding performance and particle behaviour: A comparative analysis. *Engineering and Technology Journal*, 41(07).

Appendix 1

Due to the file upload size limit in JME (25 MB), our file size is about 44 MB. Click on the link below to view the high-resolution figure file.

https://s32.picofile.com/file/8477682276/Figures_part_1_JME.docx.html

Appendix 2

Due to the file upload size limitation in JME (25 MB), click on the links below to see the high-resolution images and videos of the simulations.

https://s32.picofile.com/file/8477682318/images_Part_1_JME.rar.html

https://s32.picofile.com/file/8477682342/Videos_Part_1_JME.rar.html

بررسی اثر نوع لاینر و تعداد لیفتر بر انرژی‌های جنبشی، پتانسیل، و کل واسطه‌های آسیاکنی در آسیاهای گلوله‌ای صنعتی - بخش ۱: لیفترهای مجزا با حجم‌های یکسان

محمد جهانی چگنی*، سجاد کلاهی و اصغر عزیزی

دانشکده مهندسی معدن، نفت، و ژئوفیزیک دانشگاه صنعتی شاهرود، شاهرود، ایران

ارسال ۲۰۲۴/۰۷/۲۴، پذیرش ۲۰۲۴/۱۲/۲۸

* نویسنده مسئول مکاتبات: M.Jahani@shahroodut.ac.ir

چکیده:

انرژی مصرفی مهمترین مسئله و نگرانی در آسیاهای گلوله‌ای صنعتی است و بخش عمده‌ای از هزینه‌های کارخانه‌های فرآوری مواد معدنی را شامل می‌شود. با استفاده از لاینرهای مناسب و تعداد بهینه لیفترها، انرژی آسیا به نحو مناسبی به گلوله‌ها منتقل می‌شود. در بخش اول این کار تحقیقاتی، پنج نوع لاینر یعنی لورین، آسبورن، ریب، مکعبی و هایلر بررسی شده‌اند. این لاینرها همگی دارای لیفترهای مجزا با حجم یکسان هستند. تفاوت آن‌ها در عرض، ارتفاع و نوع پروفیل لیفتر است. ابتدا همه انواع لاینرها با استفاده از روش اجزای گسسته (راگ) با چهار بالابر شبیه‌سازی شده‌اند. سپس تعداد لیفترها چهار تا چهار تا افزایش داده شده است تا تمام جداره آسیا با لیفترها پر شود. بر این اساس لاینر لورین از ۴ تا ۲۴ لیفتر، لاینر آسبورن از ۴ تا ۱۲۰ لیفتر، لاینر ریب از ۴ تا ۴۰ لیفتر و لاینرهای مکعبی و هایلر از ۴ تا ۶۴ لیفتر شبیه‌سازی شده‌اند. برای اولین بار، انرژی جنبشی (KE) و پتانسیل (PE) و همچنین مجموع این دو انرژی (TE) همه گلوله‌ها محاسبه، و در کل مدت شبیه‌سازی از ۰ تا ۱۳ ثانیه برای همه انواع لاینرها و تعداد لیفترهای ذکر شده در بالا مقایسه شده‌اند. در نهایت با استفاده از داده‌های مربوط به PE، KE و TE برای هر نوع لاینر، تعداد بهینه لیفترها به دست آمده است. بر این اساس برای لاینر لورین ۱۶ تا ۲۰ لیفتر، برای لاینر آسبورن ۶۴ تا ۷۶ لیفتر، برای لاینر ریب ۲۴ تا ۳۲ لیفتر، برای لاینر مکعبی ۴۴ بالابر و برای لاینر هایلر ۳۶ تا ۴۴ بالابر پیشنهاد شده‌اند.

کلمات کلیدی: روش اجزای گسسته، آسیاهای گلوله‌ای صنعتی، نوع لاینر، تعداد لیفتر، انرژی‌های جنبشی، پتانسیل و کل.